energy&fuels

pubs.acs.org/EF

Article

Pore Structure Formation Mechanism of Lacustrine Fine-Grained Sedimentary System in Fengcheng Formation, Junggar Basin, China

Zaiquan Yang, Dongxia Chen,* Xianglu Tang, YuChao Wang, Zhenxue Jiang, Leilei Yang, and Zhiye Gao

Cite This: *Energy Fuels* 2025, 39, 7235−7253

Read Online

ACCESS | Metrics & More | Article Recommendations | Supporting Information

ABSTRACT: The Fengcheng Formation in the Mahu Sag of the Junggar Basin exhibits complex depositional systems containing heterogeneous hydrocarbon resources across distinct subregions. Shale oil accumulations predominantly occur in the northwestern basin sector, where significant variations in reservoir-oil-bearing potential arise from depositional heterogeneity and differential pore structure development within target intervals, presenting substantial challenges for commercial development. This study systematically investigates pore architecture and its controlling factors in Fengcheng Formation reservoirs, with a specific focus on sedimentary microfacies, mineralogical composition, and diagenetic alterations. A multidisciplinary characterization approach integrating high-pressure mercury intrusion (HPMI), low-temperature nitrogen adsorption, field emission scanning electron microscopy (FE-SEM), X-ray diffraction (XRD), and conventional petrophysical analysis was employed to evaluate reservoir characteristics across sedimentary microfacies. Key findings reveal pronounced petrophysical contrasts among microfacies: (1) displays low porosity primarily controlled by intense mechanical compaction and cementation processes, resulting in substantial pore space reduction and low permeability. (2) Tempestite microfacies: demonstrates favorable pore characteristics attributed to high-energy depositional environments and carbonate dissolution, with secondary porosity generation enhancing pore connectivity through well-developed macropore networks. (3) Quiet Water microfacies: exhibits moderate porosity but restricted permeability due to pore-throat obstruction by felsic minerals and clay authigenesis, significantly limiting fluid mobility. (4) Slump microfacies: characterized by low porosity influenced by differential compaction and complex mineralogical assemblages, it leads to poorly connected pore systems with correspondingly low permeability. This study establishes a systematic analytical framework for pore structure evaluation in heterogeneous reservoirs of the Fengcheng Formation and elucidates the critical controls exerted by sedimentary microfacies differentiation, mineralogical constraints, and diagenetic overprinting on reservoir quality evolution.

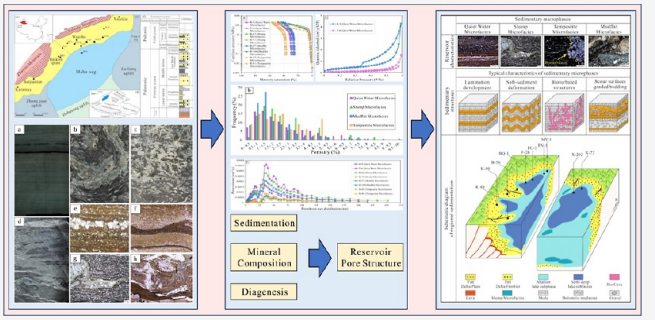

1. INTRODUCTION

Terrestrial shale oil, as an important component of unconventional oil and gas resources, has become a key focus of global exploration and development.[1−3] In contrast to marine shale oil, terrestrial shale oil reservoirs exhibit significant heterogeneity, primarily due to differences in depositional environments, pore structure characteristics, and diagenetic processes.[4−6] These variations result from the rapid changes in terrestrial depositional settings, the complexity of sedimentary materials, and the diversity of diagenetic processes.[7,8] Globally, the pore structures of terrestrial shale oil reservoirs show substantial heterogeneity. The combined effects of various depositional and diagenetic factors lead to notable differences in pore structures across different regions and stratigraphic layers, which in turn impact the occurrence and distribution of oil and gas.[9]

Compared to global advancements, China has also made substantial progress in the exploration of terrestrial shale oil.[10] Notable examples include shale oil in the Fengcheng Formation of the Mahu Depression in the Junggar Basin, Gulong shale oil in the Songliao Basin, and Chang 7 shale oil in the Ordos Basin. Among these, the Fengcheng Formation shale oil in the Junggar Basin has seen particularly significant progress.[11] As a typical terrestrial sedimentary basin, the Junggar Basin is characterized by a complex depositional system and pronounced reservoir heterogeneity.[12] The depositional environments and diagenetic processes within the Fengcheng Formation show considerable variability, which further increases the heterogeneity of the reservoir pore structures.[13] These complex sedimentary facies and diagenetic processes result in substantial variations in physical properties, such as porosity and permeability, leading to significant differences in oil saturation and production potential

Received: December 31, 2024
Revised: March 5, 2025
Accepted: March 6, 2025
Published: April 8, 2025

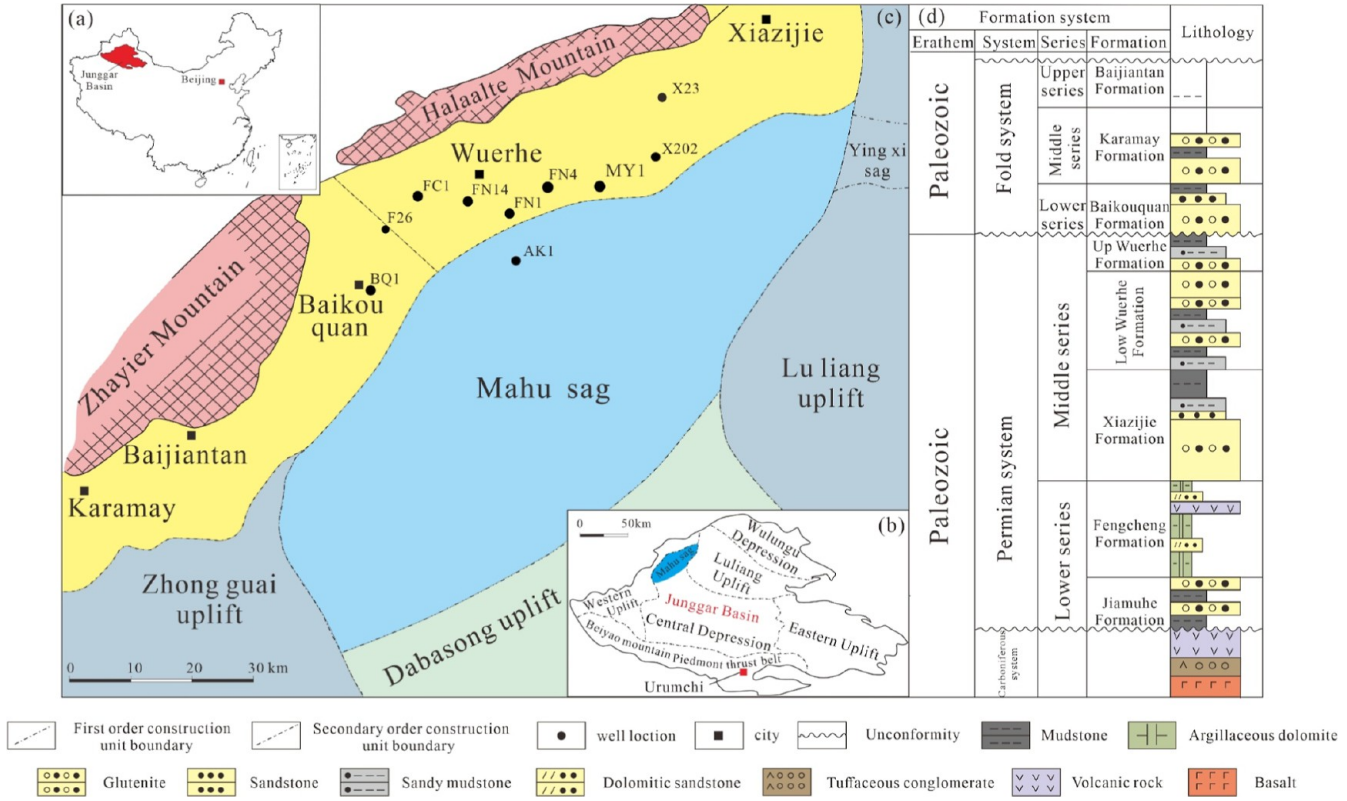

Figure 1. Structural map of Fengcheng Formation in Mahu Sag, Junggar Basin. (a) Location of Junggar Basin. (b) Location of tectonic units and study areas in Junggar Basin. (c) Location of Mahu Sag and related well positions. (d) Stratigraphic columns of Permian System in Paleozoic erathem and Triassic in mesozoic erathem.

across different target layers. This presents significant challenges for efficient exploration and development.

Although previous studies have made significant progress in understanding terrestrial sedimentary systems and diagenesis, most research has focused on individual factors, with limited comprehensive analysis of the combined effects of sedimentary microfacies and diagenesis. For example, David et al. investigated the genesis of lacustrine deposits and their controlling factors,[14] Hatano and Yoshida identified the depositional environment of lacustrine sediments through thin section analysis and field outcrops,[15] and Tang et al. characterized the structural features of lake sediments using lithologic imaging and well log data.[16] In addition, Lahann and Swarbrick modeled the transformation of montmorillonite to Illite and examined its impact on reservoir properties,[17] Liu et al. evaluated the effects of diagenetic evolution on shale reservoirs using scanning electron microscopy and micro-CT imaging,[18] and Wang et al. analyzed the influence of various diagenetic processes on pore evolution in reservoirs using conventional thin sections and electron probe analysis.[19] Clarkson et al. characterized shale pore structures with gas adsorption and small-angle neutron scattering techniques,[20] Shao et al. investigated the relationship between shale pore structure and organic matter by calculating pore fractal dimensions,[21] and Gao et al. employed scanning electron microscopy and image processing software to study the pore structure characteristics of different shale intervals.[22] However, despite these important advances in understanding individual factors, such as depositional environments, diagenesis, and pore structures, the combined effects of multiple factors, including diagenesis and mineral composition across different microfacies, on variations in pore distribution remain insufficiently explored. This limitation hinders a comprehensive understanding of pore structures in the shale reservoirs.

This study investigates the Fengcheng Formation in the Mahu Depression of the Junggar Basin. A variety of qualitative and quantitative experimental techniques, including high-pressure mercury injection (HPMI), nitrogen adsorption, scanning electron microscopy (SEM), X-ray diffraction (XRD), major and trace element analysis, and RoPscan, are employed to meticulously characterize the depositional system of the Fengcheng Formation. Based on the identified sedimentary microfacies, the study offers a detailed description of the reservoir heterogeneity across different microfacies. By integration of sedimentary processes, mineral composition, and diagenesis, this research provides a comprehensive analysis of the pore structure characteristics of the Fengcheng Formation reservoirs and the factors that govern them.

2. GEOLOGICAL BACKGROUND

The Junggar Basin is located in the northern part of Xinjiang, China, along the eastern margin of the Kazakhstan Plate.[23] It consists of six primary structural units: the Western Uplift, the Ulungur Depression, the Luliang Uplift, the Eastern Uplift, the Central Depression, and the Northern Yaoshan Foreland Thrust Belt.[24] The study area, the Mahu Depression, is situated in the western part of the Central Depression near the Haralate Mountains (Figure 1). The stratigraphy of the Mahu Depression is composed of the following formations, from bottom to top: the Permian Jiamusi Formation (P_1j), the Fengcheng Formation (P_1f), the Lower West Chiji Formation of the Middle Permian (P_2x), the Lower Wuerhe Formation (P_2w), and the Upper

https://doi.org/10.1021/acs.energyfuels.4c06392
Energy Fuels 2025, 39, 7235−7253

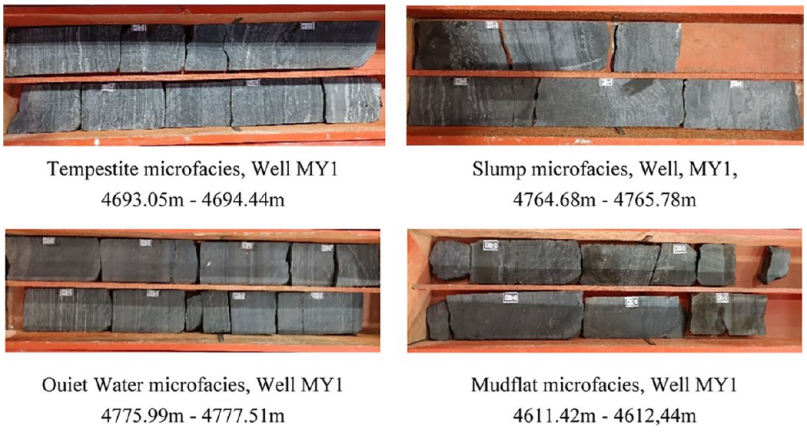

Figure 2. Cored samples of different sedimentary microfacies from well MY1.

Wuerhe Formation (P_3w).[25] The thickness of the Fengcheng Formation ranges from 800 to 1800 m and increases from the southeast to the northwest.[26] The Fengcheng Formation is divided into three members: the first member (P_1f_1), the second member (P_1f_2), and the third member (P_1f_3), each exhibiting distinct lithological characteristics.[27]

The depositional environment of the Fengcheng Formation is primarily semideep to deep lake, characterized by a complex sedimentary structure, well-developed laminations, and notable rhythmic variations, indicative of a high-salinity, reducing, arid, or semiarid climate. The formation is predominantly composed of calcareous shale interbedded with sandy reservoirs. The source-reservoir-cap rock system of the Fengcheng Formation is a typical autochthonous, self-sourced system. The cap rocks of the Fengcheng Formation are mainly mudstone and calcareous shale, which have effectively sealed the hydrocarbons, preventing their escape throughout geological history. Therefore, the Fengcheng Formation represents a classic autochthonous, self-sourced reservoir system, where the source rock, reservoir, and cap rock form a complete hydrocarbon trapping system.[28]

3. SAMPLES AND METHODS

This study focuses on the Permian Fengcheng Formation shale reservoirs with core samples collected from five key wells: MY-1, FN4, FN14, X77, and F7. A multiscale characterization approach was applied, using techniques such as HPMI, nitrogen adsorption, FE-SEM, major and trace element analysis, XRD, and conventional petrophysical tests. The samples were initially treated with a toluene/methanol distillation method to remove oil. Cylindrical samples (25 mm × 50 mm) were then prepared for petrophysical and HPMI testing, while 1 cm^3 cubic samples were used for FE-SEM analysis. The remaining samples were ground to pass through a 200-mesh sieve for nitrogen adsorption and XRD analysis. All samples were carefully petrographically described and selected prior to testing to ensure their representativeness.

The core Wells are mainly MY1 Wells. Well MY1 is a coring well with a coring depth of 4557.34−4934.73 m (Figure 2). All cores in the range of core depth are from the Fengcheng Formation. Before starting the paper work, we have a detailed description of each core of the core well. Combined with the previous investigation, the sedimentary facies types of the coring Wells in the study area have been clearly defined. Based on the previous work, we divided the sedimentary and sedimentary microfacies of the well.[29,30]

3.1. Sedimentary Microphase Identification Methods. This study primarily relies on core observation and thin section analysis for identifying the sedimentary microfacies in the Permian Fengcheng Formation shale reservoirs. Core observations, through both visual inspection and high-resolution imaging, enable direct documentation of features such as bedding, massive structures, convoluted structures, soft-sediment deformation, and bioturbation. These characteristics are used for the initial classification of microfacies types. Thin section analysis was performed by using a BX3M-LEDR transmitted/reflected optical microscope (Olympus Corporation, Japan) to examine fine structures, mineral distribution, and sedimentary lamination in greater detail. By integrating these qualitative methods with field well logging data and regional sedimentary structural characteristics, we systematically classified the sedimentary microfacies of the Fengcheng Formation, providing a petrological basis for subsequent quantitative reservoir property characterization.[31]

3.2. Reservoir Identification Methods for Different Sedimentary Microphases. This study utilized both qualitative and quantitative methods to characterize the internal pore structure of the reservoir. The qualitative methods primarily include scanning electron microscopy (SEM) and thin section analysis, which provide visual insights into the pore structure and pore size distribution of the samples. SEM imaging was performed using a Crossbeam 540 focused ion beam scanning electron microscope (Zeiss, Germany). For the quantitative analysis, high-pressure mercury injection (HPMI) and nitrogen adsorption techniques were employed.[32]

To thoroughly characterize the multiscale pore system of the Fengcheng Formation reservoir, a combined qualitative and quantitative approach was adopted. Qualitatively, FE-SEM was used to observe the microstructural features of the pores, while thin section analysis provided a detailed examination of the pore morphology and connectivity. Quantitative analysis was conducted using HPMI testing to obtain key parameters, such as pore-throat radius, pore volume fraction, and displacement pressure. Additionally, low-temperature nitrogen adsorption was applied to samples ground to 200 mesh in order to analyze the pore size distribution, compensating for the limitations of HPMI measurements in the macro- and mesopore ranges. XRD was also performed to conduct a quantitative analysis of the rock's mineral composition.[33]

3.3. Reservoir Mechanisms in Different Sedimentary Microfacies. This study investigates the reservoir formation mechanisms of the Fengcheng Formation from three key perspectives. First, core and thin section observations were used to document the bedding structures, bioturbation, and soft-sediment deformation features in the shale across different depositional systems. Additionally, XRD, major and trace element analyses, and SEM were employed to examine the distribution of quartz, feldspar, lithic fragments, carbonates, and clay minerals in various microfacies. These results suggest that variations in mineral composition influence the evolution of the pore system. To further explore the relationship between minerals and porosity, RopScan experiments were conducted to assess mineral-pore interactions. RopScan scans both porosity and mineral distribution in the rock, utilizing image analysis techniques to quantify the interactions.[34,35] This approach provides a more detailed understanding of pore evolution and enables quantitative analysis of pore structures across different depositional systems.[36]

https://doi.org/10.1021/acs.energyfuels.4c06392
Energy Fuels 2025, 39, 7235−7253

4. RESULTS

4.1. Reservoir Petrological Characteristics. As an part of a comprehensive characterization of the shale sedimentary environment, shale lithofacies can be used to reflect the color, structure, mineral composition, and organic characteristics.[37] As a consequence of complex lithologic changes and variable sedimentary structures observed in the shale members of the Fengcheng Formation, felsic, carbonate, and clay minerals were selected as three different endmembers, and as the boundaries of the lithofacies of the Fengcheng Formation, 25%, 50%, and 75% of the mineral composition were used: I-felsic shale (I_1—felsic shale, I_2—mica-diorite-bearing felsic shale, I_3—clay-bearing felsic shale), II-calcareous shale (II_1—calcareous shale, II_2—felsic calcareous shale, II_3—clay-bearing calcareous shale), III-dolomitic shale (III_1—dolomitic shale, III_2—felsic dolomitic shale, III_3—clay-bearing dolomitic shale), IV-clay shale (IV_1—clay shale, IV_2—feldspar clay shale, IV_3—ash/cloud clay shale), and so on. In Mahu Sag, felsic and dolomitic shales are primarily developed in the Fengcheng Formation (Figure 3).

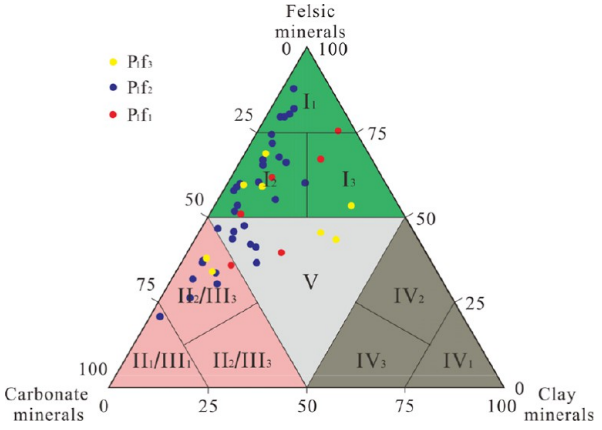

Figure 3. Lithologic division of the shale in the Fengcheng Formation. I_1—felsic shale, I_2—mica-diorite-bearing felsic shale, I_3—clay-bearing felsic shale, II_1—calcareous shale, II_2—felsic calcareous shale, II_3—clay-bearing calcareous shale, III_1—dolomitic shale, III_2—felsic dolomitic shale, III_3—clay-bearing dolomitic shale, IV_1—clay shale, IV_2—feldspar clay shale, IV_3—ash/cloud clay shale, V—mixed shale.

The sedimentary microfacies in the Fengcheng Formation primarily consist of felsic minerals, carbonate minerals, pyrite, and clay minerals. Felsic minerals make up an average of 51.3% with quartz, potassium feldspar, and plagioclase as the main components. Quartz content ranges from 26% to 49.7%, potassium feldspar from 14% to 35.9%, and plagioclase from 8.7% to 39.7%. Carbonate minerals, primarily calcite and dolomite, range from 7.8% to 26.3% for calcite and 0.5% to 19.6% for dolomite (Table 1). The mineral composition varies across different sedimentary microfacies. In the Mudflat Microfacies, clay minerals account for approximately 24.2% to 43%. In the Tempestite Microfacies, carbonate minerals are dominant, ranging from 7% to 26.3%. In the Quiet Water Microfacies, quartz and feldspar together make up about 54.9% to 64.3%. In the Slump Microfacies, carbonate minerals are the most prominent, ranging from 19.6% to 39.7% (Figure 7).

4.2. Sedimentary Microfacies: Classification and Characteristics. Based on lithology and sedimentary structures, the lacustrine depositional system of the Fengcheng Formation is divided into two subfacies: shallow lake and semideep lake subfacies. The semideep lake subfacies includes two microfacies: Quiet Water Microfacies (Figure 4a,e) are characterized by millimeter-scale rhythmic laminations formed under low-energy, oxygen-depleted conditions, with occasional weak bioturbation. This indicates that benthic biota activity was limited due to anoxic bottom water conditions. The formation of this microfacies is primarily associated with seasonal suspended sediment deposition, where alternating layers of clay and organic matter create rhythmic laminations. The anoxic environment suppresses biological disturbance, thereby preserving the primary laminations. Slump Microfacies (Figure 4b,f,g), which is formed by slope instability during codeposition, is characterized by convoluted bedding and soft-sediment deformation structures. In this microfacies, shear fractures and liquefaction processes generate a fracture network that locally enhances pore connectivity. However, the disruption of primary laminations significantly reduces reservoir homogeneity. Slump formation is typically linked to seismic activity or rapid sedimentation, both of which trigger slope instability and cause plastic deformation of the sediments before full consolidation.

The shallow lake subfacies consist of two microfacies: tempestite microfacies (Figure 4d), characterized by thick, massive bioclastic sandstone and hummocky cross-stratification. These features indicate the deposition during high-energy storm events. During such events, strong wave and backflow actions transport coarse materials to shallow lake areas, where rapid deposition results in thick, massive beds. The hummocky cross-stratification reflects the oscillatory flow of storm waves with coarse-grained structures dominating the formation of millimeter-scale intergranular pores. Mudflat Microfacies (Figure 4c,h), which forms in intermittently exposed, low-energy environments, is marked by bioturbated massive structures and discontinuous laminations caused by oxidation. Intense

Table 1. Mineral Composition of Fengcheng Formation Reservoir in Mahu Sag

number	depth/m	microfacies	quartz/%	feldspar/%	carbonate/%	clay minerals/%	pyrite/%
1	4588.48	mudfat	35.6	17.5	11.8	24.2	0.9
2	4590.50	mudfat	43	14	22	11	0.2
3	4592.84	mudfat	29	33	10	13	3
4	4583.65	tempestite	25	34	7	17	1
5	4585.59	tempestite	30	29	13	15	0.5
6	4606.54	tempestite	49	14	21	11	2
7	4846.64	quiet water	26	33.9	26.3	5	7.8
8	4850.43	quiet water	30.4	30.9	16.8	9.2	7.6
9	4597.30	slump	37	26	20	8	3
10	4690.85	slump	39.7	27.9	19.6	2.3	8.9

https://doi.org/10.1021/acs.energyfuels.4c06392
Energy Fuels 2025, 39, 7235−7253

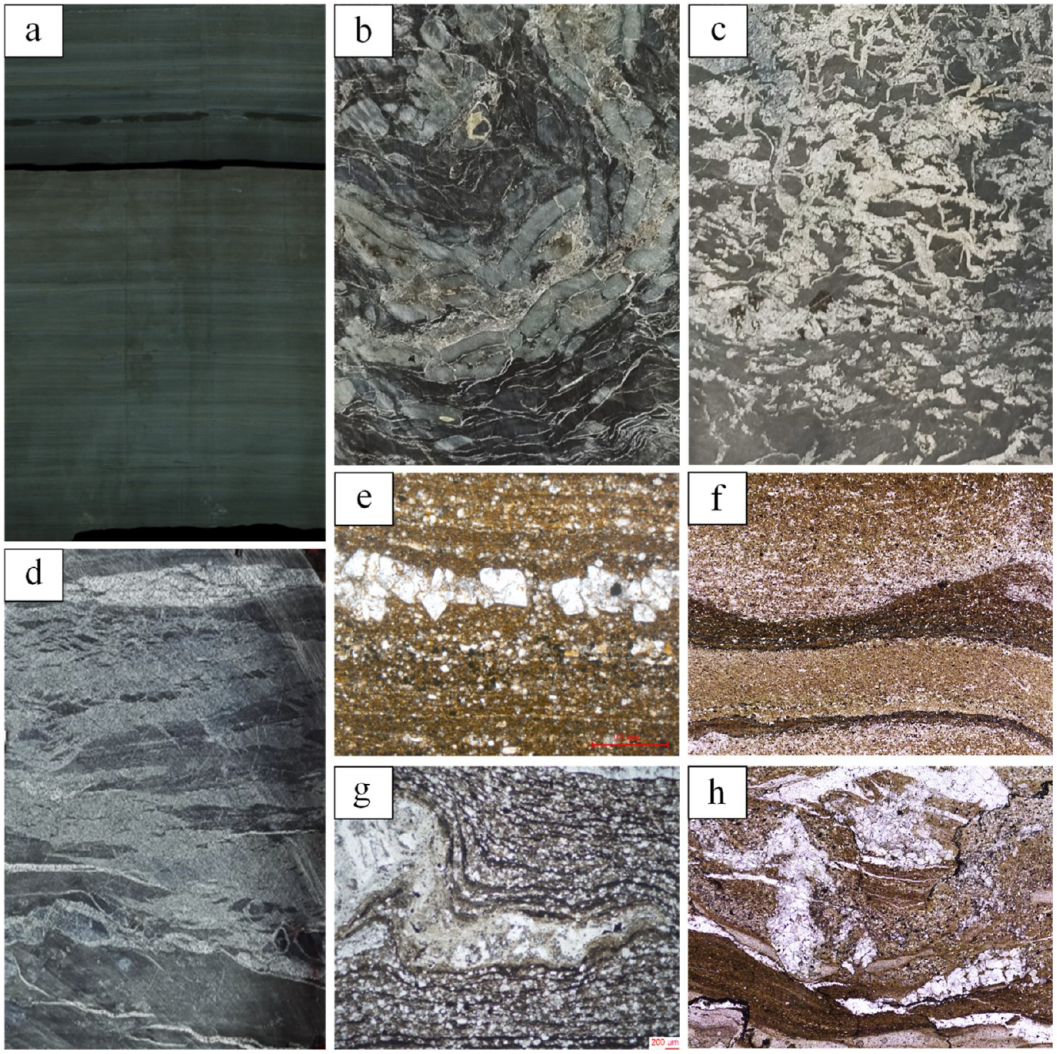

Figure 4. Lithologic photographs and facies markers of sedimentary microfacies of Permian Fengcheng Formation reservoir in Mahu Sag. (a) FN-4-4876.69 m, Quiet Water Microfacies, thinly laminated structure; (b) MY-1-4695.88 m, Slump Microfacies, convolute structure; (c) MY-1-4821.97 m, Mudflat Microfacies, bioturbated structure; (d) MY-1-4641.23 m, Tempestite Microfacies, cross-bedding structure; (e) F-7-3187.45 m, Quiet Water Microfacies, thinly laminated structure; (f) MY-1-4779.98 m, slump Microfacies, soft sediment deformation structure; (g) MY-1-4765.35 m, slump Microfacies, convolute structure; (h) MY-1-4810.97 m, mudflat microfacies, bioturbated structure.

bioturbation in these microfacies creates a mixed pore system, while the oxidation during exposure limits the development of organic-rich porosity, thereby increasing the heterogeneity of the reservoir.

Both the Quiet Water and Tempestite Microfacies exhibit high gamma ray (GR) values and moderate to low resistivity in well logging data, while the Slump and Mudflat Microfacies display moderate GR values. According to the sedimentary microfacies distribution for well MY-1, the lower portion of P_1f_1 is predominantly composed of Quiet Water Microfacies. In P_1f_2, the lower water column gradually becomes shallower, revealing Mudflat Microfacies along with a mixture of Slump and Quiet Water Microfacies. In the upper part of P_1f_2, as the water deepens, the sedimentary microfacies undergo a transition from Mudflat to Quiet Water Microfacies. In the lower part of P_1f_3, the water column shallows again and the stronger hydrodynamic conditions lead to the development of Tempestite Microfacies. In the upper part of P_1f_3, as the water deepens, Quiet Water Microfacies prevail. Overall, the Fengcheng Formation is primarily dominated by Quiet Water and Mudflat Microfacies, with localized occurrences of Slump and Tempestite Microfacies (Figure 5).

The sedimentary system of the Fengcheng Formation exhibits a distinct transition from the basin margin to the basin center with increasing water depth and decreasing grain size. At the basin margin, a deltaic depositional system, predominantly composed of coarse-grained clastics, is developed. The sediments primarily originate from the erosion and transport of surrounding mountain ranges, featuring river channel sand bodies, deltaic bars, and foreset beds deposited under high-energy conditions. As the depositional environment shifts toward the basin center, it transitions into a low-energy lacustrine system, dominated by fine-grained mudstones and siltstone-rich mudstones. This facies is characterized by horizontal bedding, seasonal laminations, and bioturbation, reflecting stable, quiet-water conditions. From P_1f_1 to P_1f_3, as the lake level rises, the lake basin expands significantly, with the sedimentary center gradually migrating from the north to the northwest and southwest (Figure 6).

4.3. Sedimentary Microfacies: Reservoir Physical Property. Based on the classification of sedimentary

https://doi.org/10.1021/acs.energyfuels.4c06392
Energy Fuels 2025, 39, 7235−7253

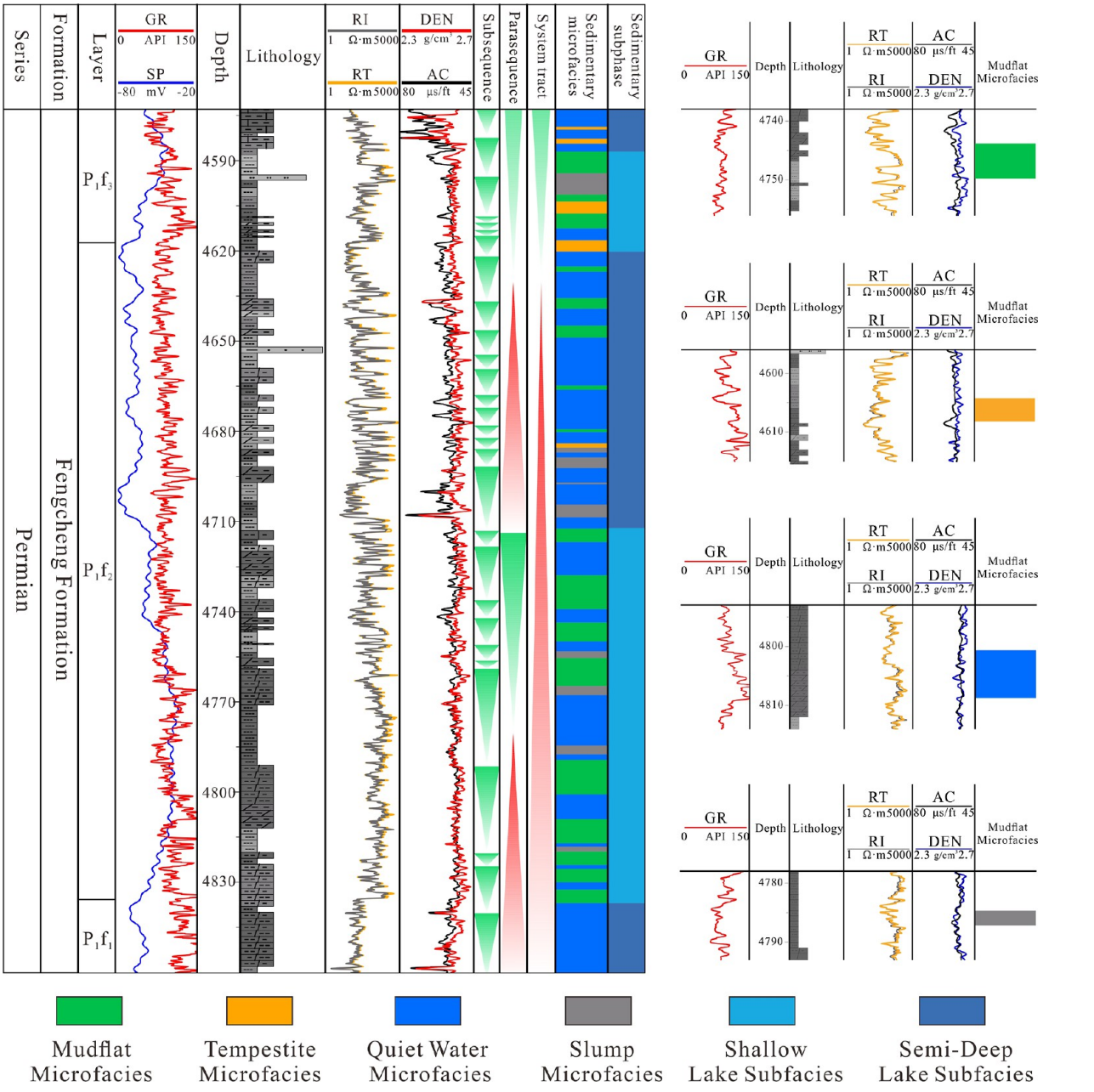

Figure 5. Distribution characteristics of sedimentary microfacies in a single well of the Fengcheng Formation, MY-1.

microfacies in the Fengcheng Formation, we conducted a detailed analysis of the petrophysical properties of each microfacies. Significant differences in porosity and permeability were observed across the sedimentary microfacies. Overall, the Quiet Water Microfacies has relatively high porosity, typically ranging from 1 to 6%, with permeability showing considerable variation. While some samples exhibit higher permeability, most samples show low permeability, which suggests that although the pores are larger, their poor connectivity restricts fluid flow. The Tempestite Microfacies generally exhibit low porosity, ranging from 0.1 to 2.5%, and also display low permeability. Most data fall within the 0.01−0.1 mD range, indicating that the Tempestite Microfacies has relatively poor reservoir quality, with both porosity and permeability at lower levels (Figure 7).

The Mudflat Microfacies shows a broad range of porosity, from 0.4 to 8.8%, with most values concentrated in the lower porosity range. Permeability is predominantly low, indicating that the reservoir capacity in most areas of these microfacies is weak. The Slump Microfacies has porosity ranging from 0.5 to 8.2%. Although some samples exhibit relatively high porosity, permeability is generally low, suggesting that while this microfacies has larger pore spaces, poor pore connectivity results in lower fluid flow capacity. Overall, these findings indicate that the grain size, depositional environment, and pore structure are critical factors influencing porosity and permeability.

4.4. Sedimentary Microfacies: Reservoir Pore Structure Characteristics. The pore structures of the Fengcheng Formation vary across different sedimentary microfacies due to differences in mineral composition, burial depth, and diagenetic processes. In the Quiet Water Microfacies, the pore system consists primarily of irregular primary intergranular pores and narrow intergranular pores with localized pyrite and elliptical dissolution pores (Figure 8A,C). The Slump Microfacies are

https://doi.org/10.1021/acs.energyfuels.4c06392
Energy Fuels 2025, 39, 7235−7253

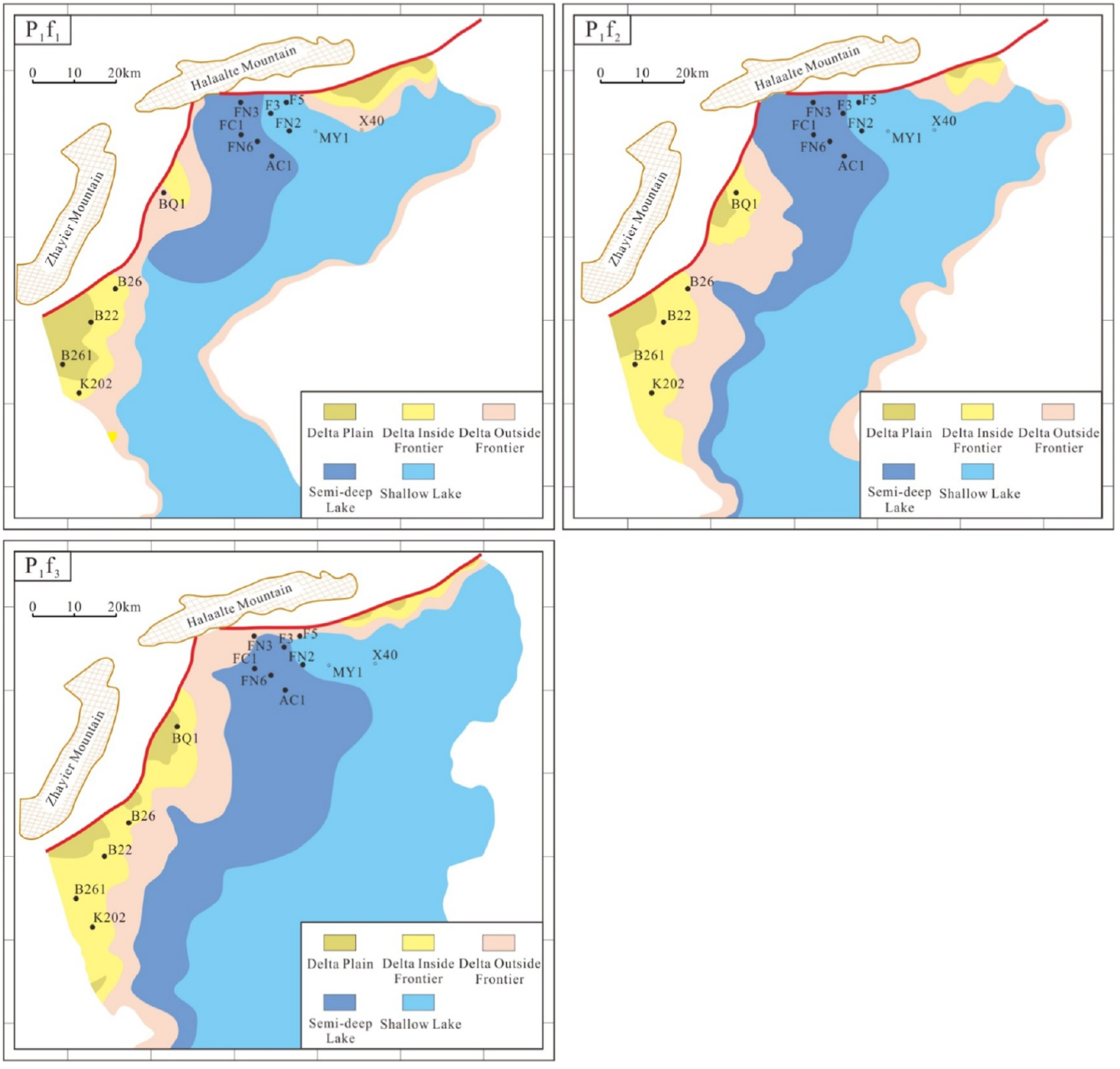

Figure 6. Distribution of sedimentary microfacies across the three segments of the Fengcheng Formation.

characterized by triangular and wedge-shaped intergranular pores, with less development of organic pores (Figure 8H,I). In the Mudflat Microfacies, slit intergranular pores, predominantly composed of clay minerals, are the dominant pore type with organic and intragranular pores poorly developed (Figure 8D). The Tempestite Microfacies exhibits a prominent presence of intergranular and intragranular pores, with relatively well-developed organic matter pores, contributing to a more complex and interconnected pore network (Figure 8E,F, and G).

These differences in pore structures reflect variations in the depositional environments and diagenetic processes of the microfacies. Organic matter pores in the Fengcheng Formation are less developed compared to those found in marine shales in China, particularly those in advanced maturity or overmaturity stages. The predominant pore types in the Fengcheng Formation are intergranular and intragranular pores, with organic matter pores being more pronounced in the Tempestite Microfacies (Figure 8B,E). These differences underscore the critical influence of depositional conditions and diagenesis on the development of pore systems in the Fengcheng Formation.

4.5. Sedimentary Microfacies: Reservoir Pore Size Distribution Characteristics. High-pressure mercury injection (HPMI) tests show distinct pore-throat radius characteristics across different microfacies. In the Quiet Water Microfacies, mercury saturation is zero in the high-radius range. As the pore-throat size decreases to the 50−40 nm range, the mercury saturation difference increases, indicating a relatively homogeneous pore system dominated by larger pore throats, with a lower proportion of fine pores. In contrast, the Slump Microfacies shows a marked increase in mercury saturation difference within the medium to small pore diameter range, suggesting that small pore throats dominate this microfacies. As a result, the pore volume is concentrated in the smaller pore diameter range, which could limit fluid

https://doi.org/10.1021/acs.energyfuels.4c06392
Energy Fuels 2025, 39, 7235−7253

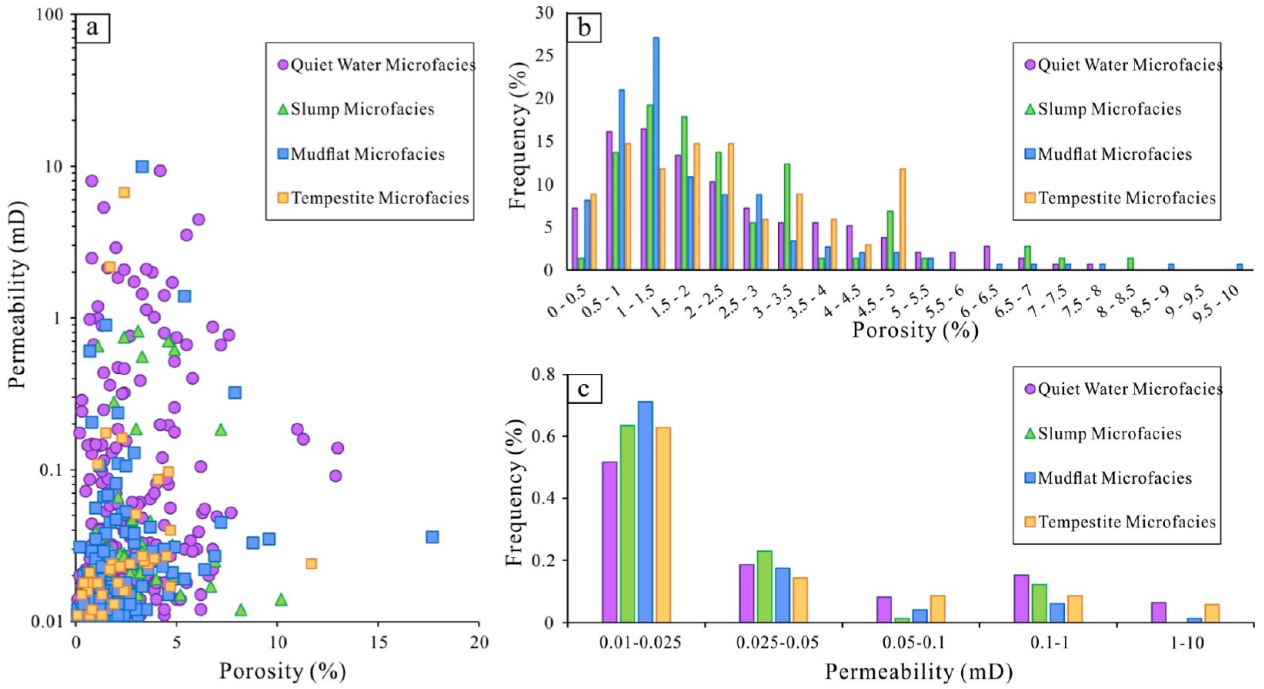

Figure 7. (a) Relationship between porosity and permeability of reservoirs in different sedimentary microfacies of the Fengcheng Formation; (b) histogram of porosity distribution for reservoirs in different microfacies; (c) histogram of permeability distribution for reservoirs in different microfacies.

connectivity. The Mudflat Microfacies display a wide distribution of pore-throat radii, with significant variation in mercury saturation in the low-pore diameter region, reflecting considerable heterogeneity in the pore structure. In certain areas, intense compaction and cementation may lead to a more compact pore system. The Tempestite Microfacies, on the other hand, shows higher mercury saturation in the low-pore diameter range, while maintaining relatively low mercury saturation in the larger pore-throat range (30−50 nm). This suggests that the Tempestite Microfacies contains both fine pores and well-developed mesopores or macropores, which facilitate fluid flow and enhance reservoir properties (Figure 9).

Nitrogen adsorption data complement the limitations of HPMI in characterizing the pore size distribution in shale. By incorporating pore volume distribution as an additional measure, these data provide deeper insight into the pore volume characteristics of each sedimentary microfacies across different pore diameter ranges. The Quiet Water Microfacies show a minimal increase in pore volume in the lower pore diameter range, indicating a relatively uniform pore structure with limited micropore development. The Slump Microfacies exhibits a moderate increase in pore volume in the medium to small pore diameter range, suggesting a mix of micropores and some mesopores, although the overall pore volume remains relatively low. The Mudflat Microfacies reveal a sharp increase in pore volume in the medium to large pore diameter range, indicating significant heterogeneity in the pore structure. This is likely related to the secondary porosity formed by localized dissolution under intense compaction and cementation. The Tempestite Microfacies displays a complex pore volume distribution, with a gradual increase in micropores in the lower pore diameter range and a prominent peak in pore volume at larger pore diameters. This combination of pore sizes provides both storage capacity and enhanced fluid flow potential (Figure 10).

5. DISCUSSION

5.1. Effect of Sedimentation on Reservoir Properties.

The influence of sedimentary processes on reservoir properties is primarily reflected in how ancient depositional environments have shaped the characteristics of microfacies in the target layers. Variations between microfacies lead to differences in reservoir properties within the vertical profile of the Fengcheng Formation. This study investigates the effects of depositional environment factors, including ancient water depth, salinity, and redox conditions, on sedimentary microfacies and how these factors influence the petrophysical differences across microfacies.

Ancient water depth impacts hydrodynamic conditions and the position of redox interfaces, influencing sediment types and the spatial distribution of microfacies. Shallow water environments, affected by wave and storm waves, experience strong hydrodynamic conditions, which favor the formation of Tempestite Microfacies. In these microfacies, high-energy currents scour the seabed, depositing coarse clastics such as quartz and feldspar, forming cross-bedded sandstones.[37] This high-energy environment leads to higher initial porosity, but subsequent silica cementation significantly occludes pore throats, reducing pore connectivity and resulting in relatively low permeability. In deeper water environments, located below the storm wave base, low-energy, continuous deposition predominates, promoting the formation of Quiet Water Microfacies. In these microfacies, suspended loads dominate, with clay minerals and organic matter settling by gravity, forming millimeter-scale laminations (Figure 11). Permanent anoxic conditions in deeper water areas, caused by water column stratification, promote sulfate-reducing bacteria activity, leading to H_2S accumulation and pyrite formation, which further enhances organic matter preservation.[38] The strawberry-like aggregates of pyrite inhibit compaction, preserving primary

https://doi.org/10.1021/acs.energyfuels.4c06392
Energy Fuels 2025, 39, 7235−7253

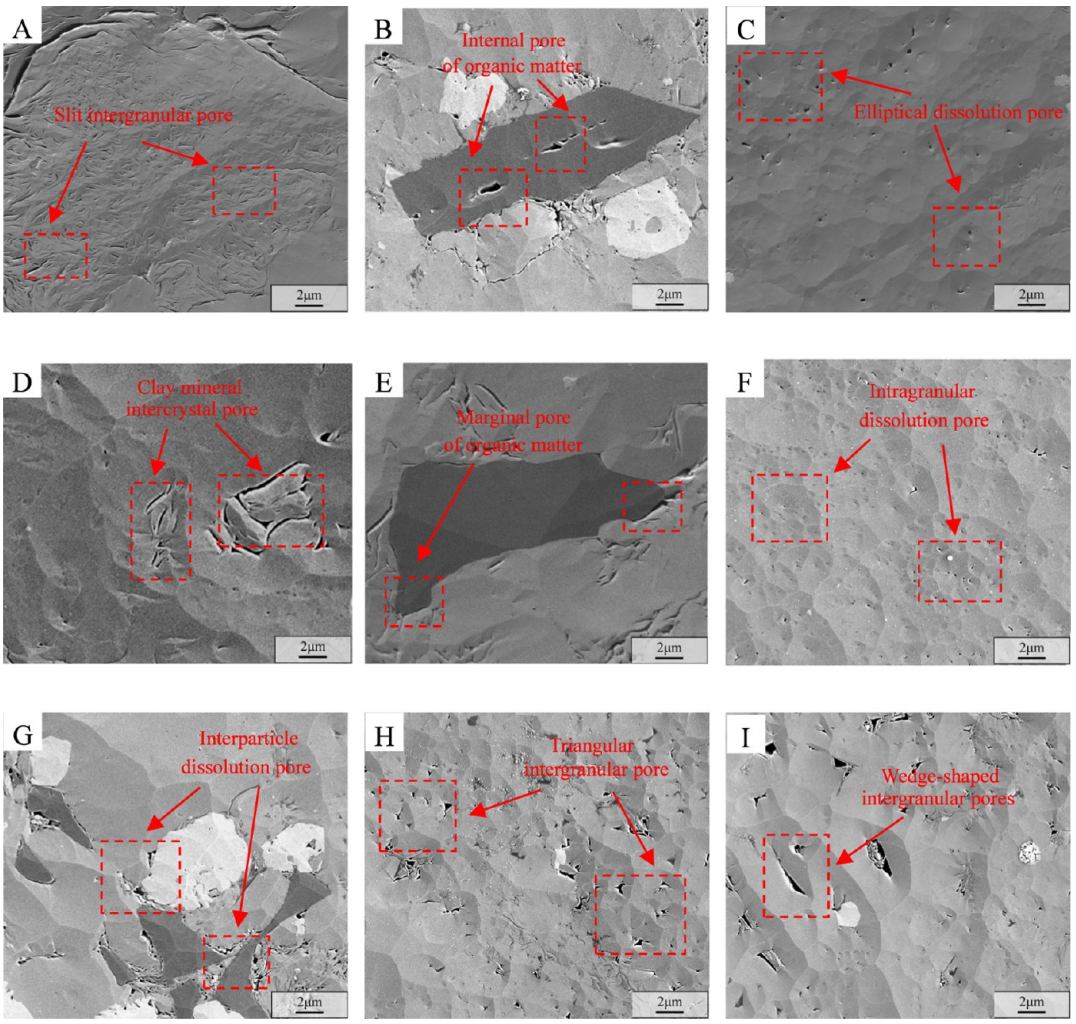

Figure 8. Types of pores that occur in different sedimentary microfacies (A) Quiet Water microfacies, MY1, 4857.57 m. (B) Tempestite microfacies, MY1, 4755.67 m. (C) Quiet Water microfacies, Elliptical dissolution pore, MY1, 4857.57 m. (D) Mudflat microfacies, MY1, 4587.92 m. (E) Tempestite microfacies, MY1, 4755.67 m. (F) Tempestite microfacies, MY1, 4755.67 m. (G) Tempestite microfacies, MY1, 4755.67 m. (H) Slumping microfacies, MY1, 4846.57 m. (I) Slumping microfacies, MY1, 4846.57 m.

porosity, which results in higher porosity and permeability in the Quiet Water Microfacies compared to other microfacies.

Ancient salinity affects mineral saturation and the structure of biological communities, thus influencing sediment chemistry and microfacies types. In high-salinity environments (Sr/Ba >1), the higher Mg/Ca ratio in lake water triggers dolomitization, forming laminated dolomitic shale (Figure 11). The intercrystalline and dissolution pores of dolomite provide additional storage space for the Quiet Water Microfacies, significantly enhancing porosity. At the same time, high salinity suppresses terrigenous clastic input, reducing quartz content and decreasing the structural support rigid particles provide to pore spaces. In low-salinity environments (Sr/Ba <0.6), freshwater influx lowers ion activity, promoting the biogenic formation of siliceous layers (Figure 11). Increased terrigenous clay input elevates Al_2O_3 content, and the interlayer pores of clay minerals, along with micropores in biogenic silica, contribute to pore development in the Mudflat Microfacies.[39] However, the plastic deformation of clay minerals during diagenesis reduces pore connectivity, resulting in relatively low permeability in the Mudflat Microfacies.

The overall sedimentary environment of the Fengcheng Formation is characterized by weak oxidative conditions, which significantly influence the preservation potential and pore characteristics of different microfacies by regulating organic matter degradation pathways and the formation of authigenic minerals. In weak oxidative environments, organic matter in the Mudflat and Tempestite Microfacies is partially degraded with Fe^{3+} occurring as hematite and Mn accumulating in the form of MnO_2 nodules. Although typical reddish-brown rocks are not found in the shallow lake facies, weak oxidative conditions still result in poor organic matter preservation, with intergranular pores being dominant. However, hematite cementation reduces pore connectivity, leading to generally lower permeability in the Tempestite Microfacies. In weakly reducing environments, anoxic conditions in the Quiet Water Microfacies promote the partial degradation of organic matter by sulfate-reducing bacteria, generating H_2S and triggering pyrite formation. Pyrite occurs in strawberry-like aggregates or as dispersed primary particles (Figure 11) and is found in both shallow and semideep lake facies. The formation of pyrite inhibits compaction, preserving the primary porosity. In the Quiet Water Microfacies, thermal maturation of organic matter generates numerous intraparticle pores, while intergranular dissolution pores are relatively scarce, likely due to the alkaline environment inhibiting the dissolution of carbonate minerals. In the Slump

https://doi.org/10.1021/acs.energyfuels.4c06392
Energy Fuels 2025, 39, 7235−7253

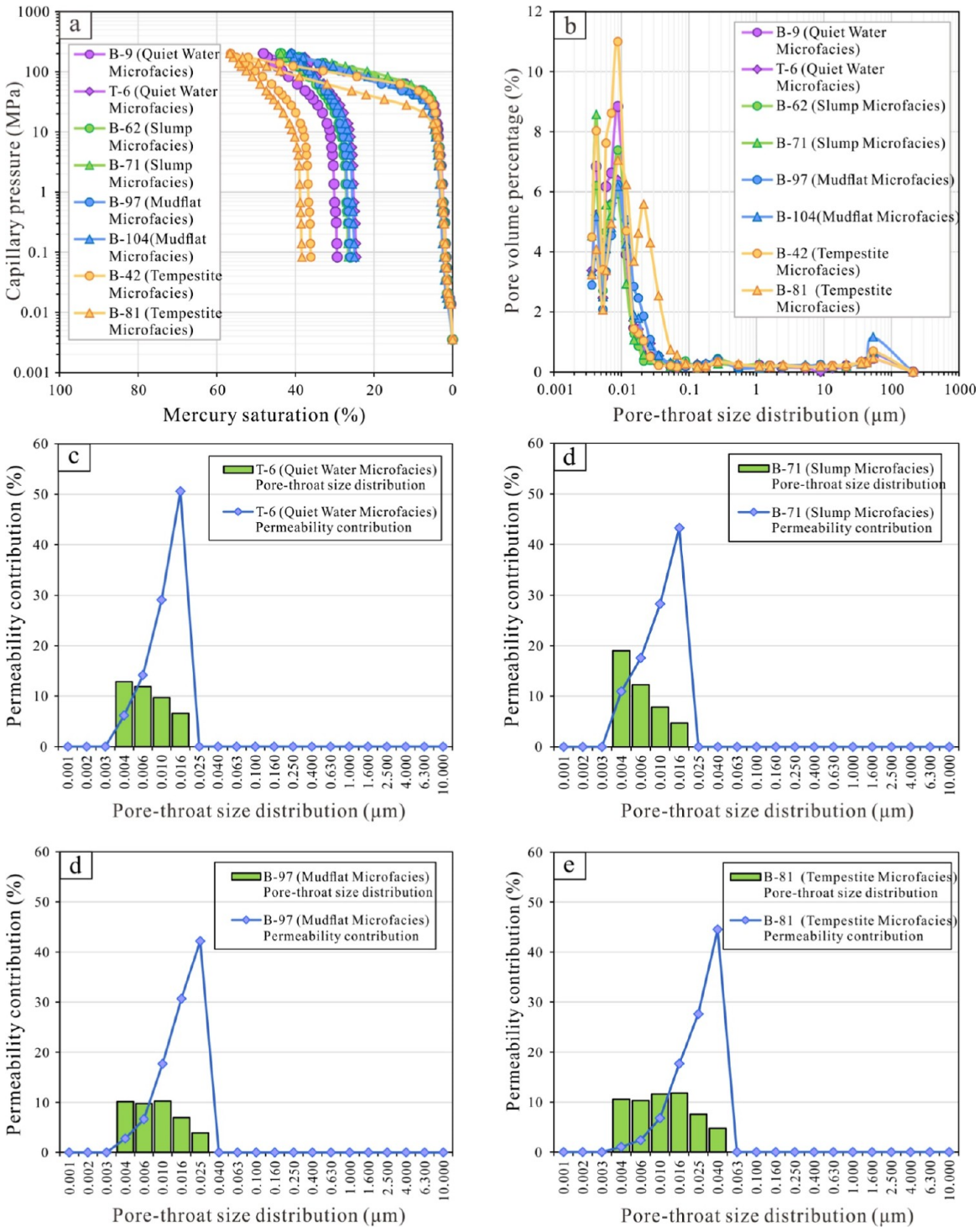

Figure 9. (a) Mercury injection and withdrawal curves from high-pressure mercury intrusion; (b) pore size distribution; (c–f) correlation between pore throat structure distribution and permeability contribution.

Microfacies, rapid sediment burial forms a poorly compacted zone, and pore fluid overpressure triggers slope instability. During slumping, organic matter and clay minerals experience a shear-induced orientation, forming deformed laminations. Microfractures generated by slumping locally improve permeability, but compaction of the plastic clay matrix reduces overall porosity, resulting in the reservoir properties of the Slump Microfacies being intermediate between those of the Quiet Water and Tempestite Microfacies.

5.2. Impact of Mineral Composition on Reservoirs. The pore structure characteristics and mineral composition of different sedimentary microfacies in the Fengcheng Formation exhibit significant variations, shaped by the depositional environment, mineral content, and postdepositional diagenesis. The Quiet Water Microfacies typically display higher porosity and a more uniform pore structure; however, their permeability is relatively low due to the influence of mineral composition. Specifically, the presence of feldspathic and clay minerals has a

https://doi.org/10.1021/acs.energyfuels.4c06392
Energy Fuels 2025, 39, 7235−7253

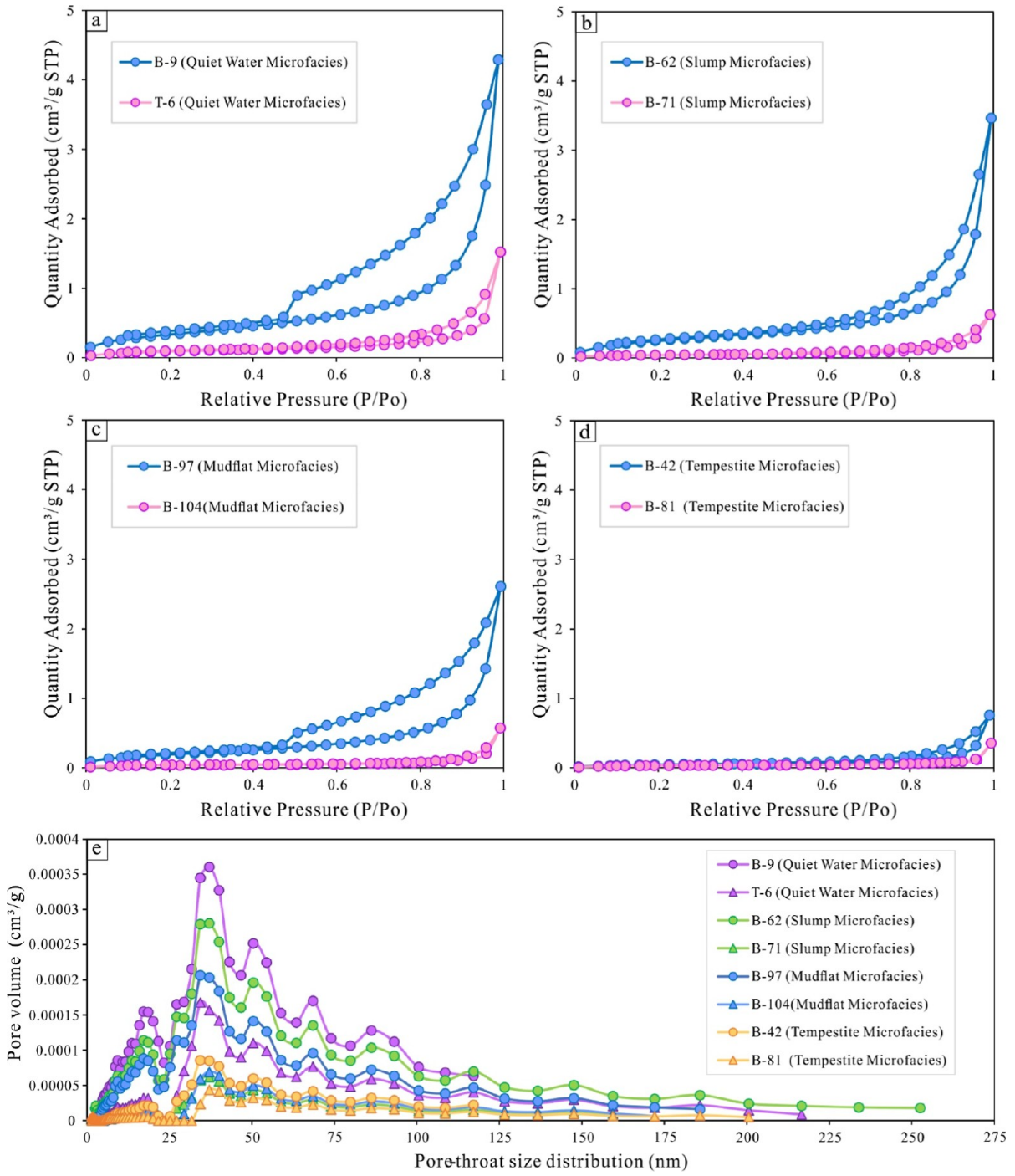

Figure 10. (a−d) Adsorption and desorption curves for the Fengcheng Formation; (e) pore size distribution.

noticeable negative effect on both porosity and permeability (Figure 12a,e). As the content of feldspathic and clay minerals increases, the volume of mesopores and macropores in feldspathic minerals decreases, while the accumulation of clay minerals fills and compacts the pore space, leading to reductions in both porosity and pore connectivity (Figure 12a,e, and f). Clay minerals, being soft particles, contribute to the development of a compact pore structure through compaction, restricting fluid flow. This suggests that while the Quiet Water Microfacies contains relatively large pore spaces, its low permeability and poor reservoir quality are primarily due to the limited pore connectivity.

In contrast to the Quiet Water Microfacies, the Tempestite Microfacies display superior reservoir characteristics with more favorable pore features. Formed in high-energy environments, the Tempestite Microfacies are typically associated with coarse-grained sediment deposition, which results in higher porosity and a greater volume of macropores. Carbonate minerals play a significant role in this microfacies (Figure 12C), with a positive correlation observed between the abundance of carbonate minerals and mesopore volume. As the content of carbonate minerals increases, the mesopore volume in the Tempestite Microfacies also increases. Furthermore, the dissolution of carbonate minerals during diagenesis creates secondary

https://doi.org/10.1021/acs.energyfuels.4c06392
Energy Fuels 2025, 39, 7235−7253

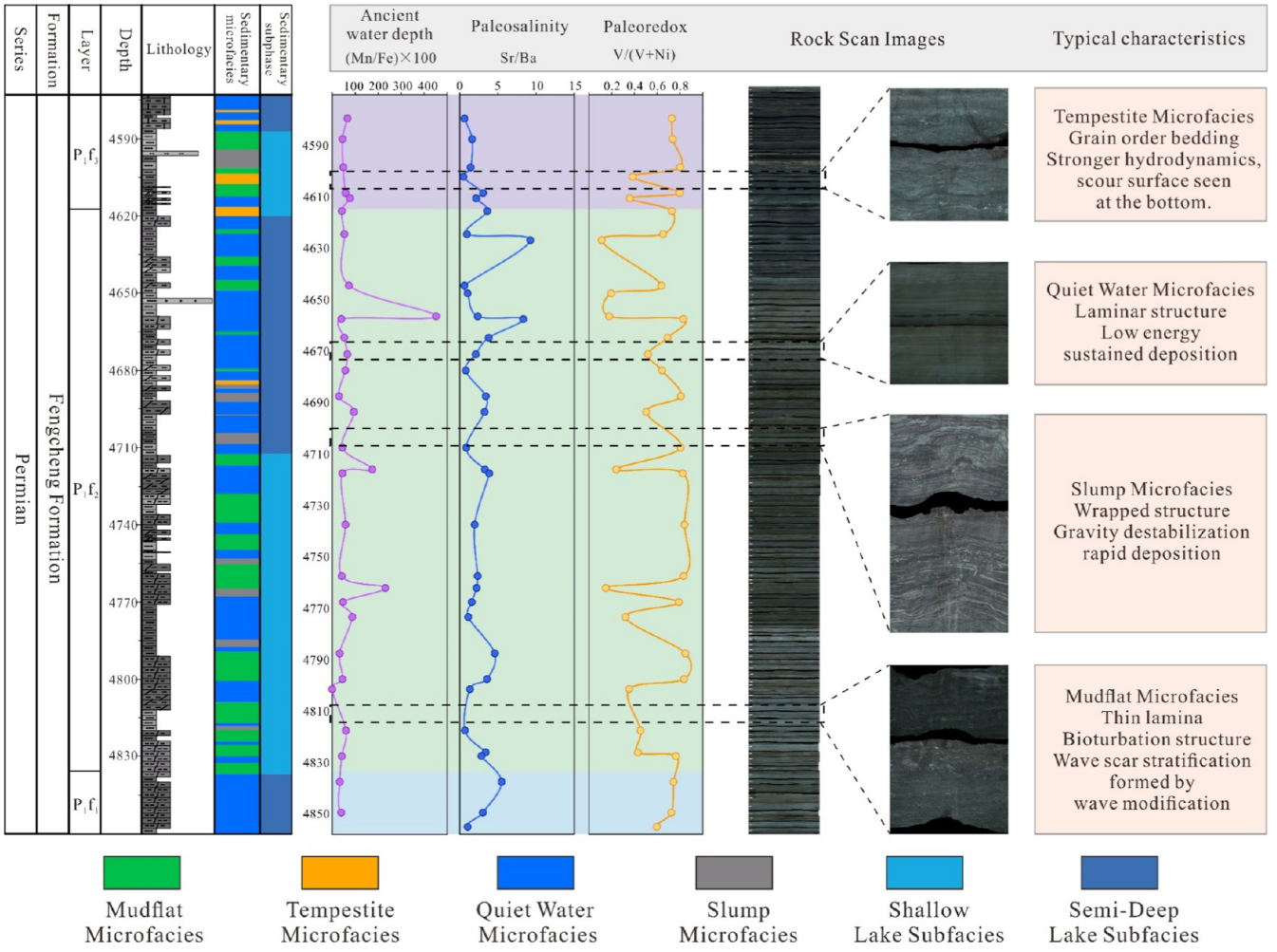

Figure 11. Comprehensive evolution diagram of sedimentary environment and sedimentary microfacies in a single well of the fengcheng formation.

porosity, improving the pore connectivity. Strong wave and backflow currents during deposition lead to a more complex pore structure, containing not only smaller pores but also well-developed mesopore and macropore channels. These features facilitate fluid flow and enhance the reservoir quality. As a result, the Tempestite Microfacies demonstrate excellent reservoir performance, with high porosity, good permeability, and strong pore connectivity.

The Mudflat and Slump Microfacies exhibit lower porosity and permeability. The Mudflat Microfacies generally form in low-energy environments and are influenced by bioturbation, resulting in a relatively dense pore structure. Specifically, the high clay mineral content in the Mudflat Microfacies promotes significant cementation and pore infilling, leading to a considerable loss of pore space and consequently, lower porosity and permeability (Figure 12e). Although the Slump Microfacies show relatively larger porosity in some areas, its porosity and permeability are limited due to compaction during deposition. The mineral composition of the Slump Microfacies is typically complex, with clay minerals playing a key role in cementation during compaction, leading to a denser pore structure and reduced pore connectivity.

To further investigate the impact of mineral composition on porosity, we combined extracted pore images with RopScan images. First, scanning electron microscope (SEM) images from samples of different sedimentary microfacies were imported into Avizo software, where the pore structures were extracted in binary form, with pores represented in black. The mineral analysis regions were subjected to a 40% blur filter, and the pore extraction results were overlaid with the mineral composition images. In the overlaid images, tonal differences between minerals were distinguished based on RGB values. These images were then imported into Photoshop for statistical analysis of the RGB values. By calculating the pore area corresponding to different RGB values, we determined the proportion of pores associated with each mineral. The results showed that quartz and feldspar have significantly greater pore-forming potential compared to dolomite and clay minerals, confirming the influence of mineral composition on pore formation and emphasizing the more prominent role of quartz and feldspar in pore generation (Figure 13).

5.3. Impact of Diagenesis on Pore Structure. *5.3.1. Impact of Compaction on Reservoir Pore Structure.* Compaction is the primary physical diagnostic process during sediment burial. It involves the application of external forces from overlying sediment and regional tectonic stress, which compress primary pores, deform particles, and result in a more compact arrangement of particles.[40] As a result, porosity decreases, and pore throat sizes shrink. The sedimentary microfacies in the Fengcheng Formation exhibit distinct responses to compaction. According to petrophysical data, the Quiet Water Microfacies (depths 4858.41 m, 4776.66 m) has effective porosity values of

https://doi.org/10.1021/acs.energyfuels.4c06392
Energy Fuels 2025, 39, 7235−7253

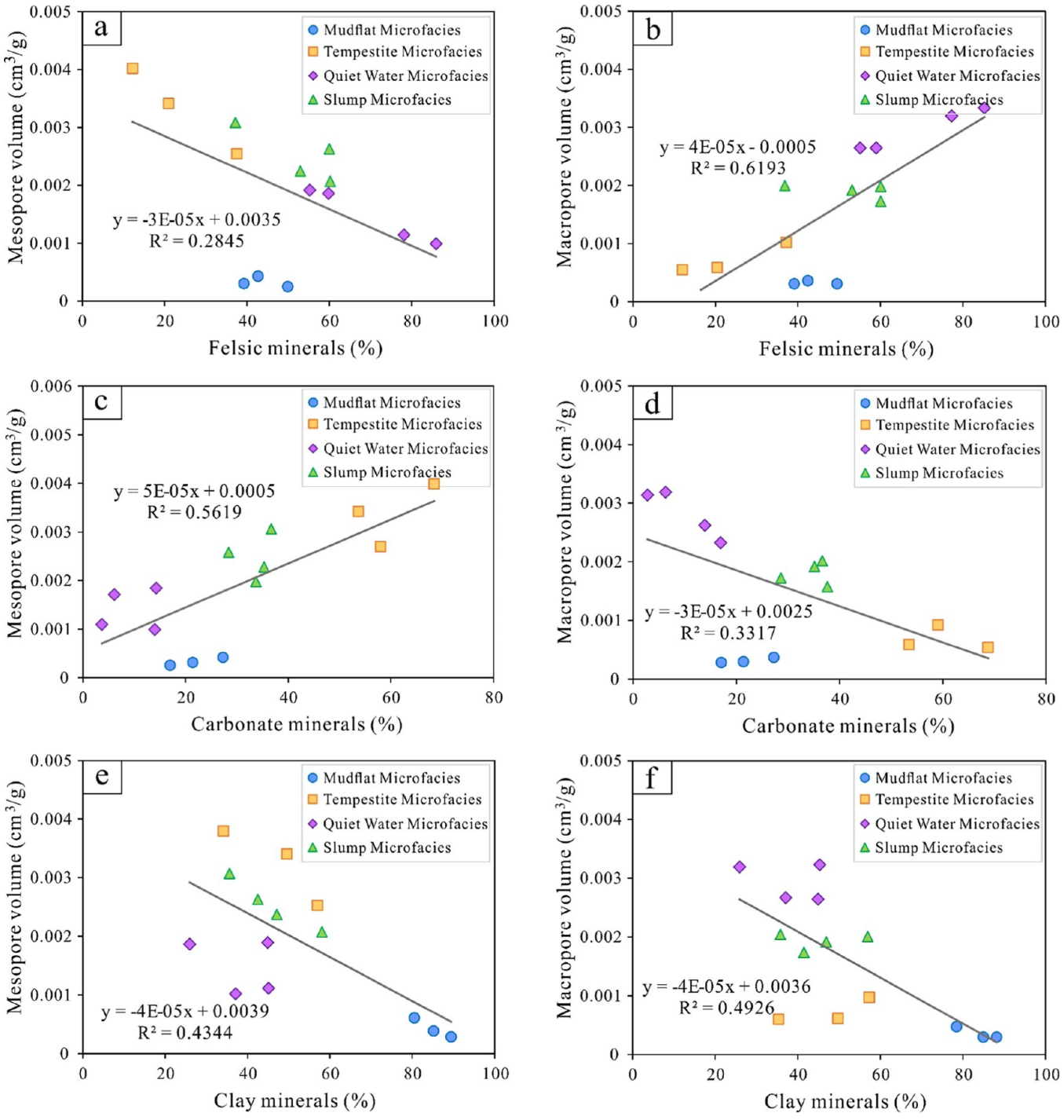

Figure 12. Relationship between shale pore volume and mineral content in different lithofacies of Fengcheng Formation.

approximately 3.27% and 1.90%, with permeability on the order of 1×10^{-4} mD. The maximum pore throat radius is around 0.021 mm, and the average pore throat radius is about 0.008 mm. Displacement pressures stabilize at around 34 MPa. These findings indicate that although fine-grained materials dominate in low-energy depositional environments, the particle-supporting structure can still partially resist compaction, preserving some porosity. However, the Quiet Water Microfacies still demonstrate poor pore connectivity due to compaction. In contrast, the Mudflat and Slump Microfacies more clearly reflect the strong impact of compaction. The Mudflat Microfacies (depths 4591.66 and 4829.15 m) have porosity values lower than 1.2%, extremely low permeability, and relatively high displacement pressures around 41 MPa. Some samples exhibit lower displacement pressures around 27.55 MPa, indicating that the fine-grained content and increased cementation tendencies cause a rapid loss of pore space during compaction. The Slump Microfacies (depths 4690.85 and 4709.68 m) show porosity between 1.61% and 1.69%, extremely low permeability, and displacement pressures around 41 MPa, suggesting that particle rearrangement following disturbance results in significant compression of primary porosity during burial. XRD data show that the mineral composition of different microfacies also influences the compaction sensitivity. The Mudflat Microfacies

https://doi.org/10.1021/acs.energyfuels.4c06392
Energy Fuels 2025, 39, 7235−7253

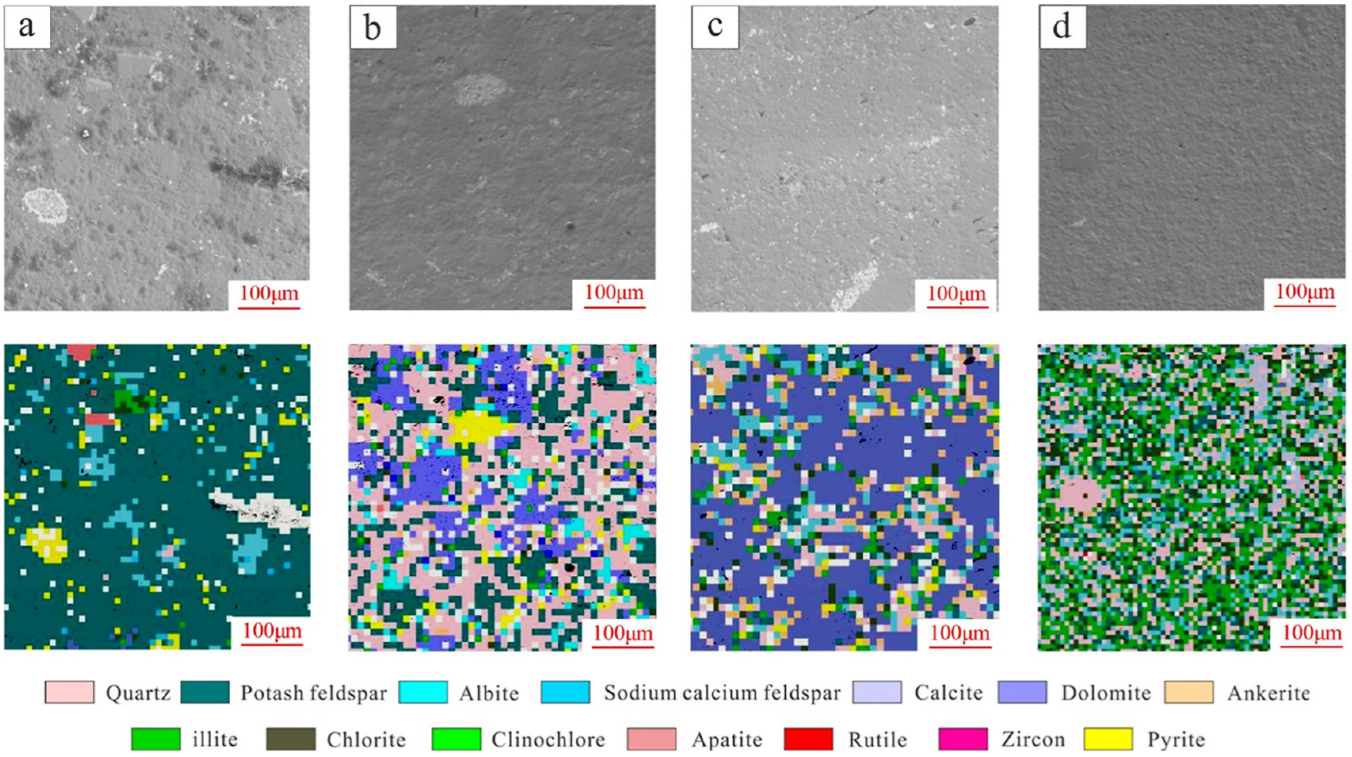

Figure 13. Common results of the superposition of mineral components with different microfacies and pores (a) Slump Microfacies, (b) Quiet Water Microfacies, (c) Tempestite Microfacies, (d) Mudflat Microfacies.

generally have a higher clay mineral content (8−14%), whereas the Quiet Water Microfacies contain more quartz and feldspar. These minerals provide better mechanical support to the particles, resulting in reduced porosity due to compaction but preserving some rigidity in the Quiet Water Microfacies, even at the same burial depth (Figure 14).

5.3.2. Impact of Cementation on Reservoir Pore Structure. Clay minerals, as common fine-grained components in sediments, not only constitute the sediment matrix but also significantly influence diagenesis by filling intergranular pores through cementation, thereby affecting reservoir properties.[41] The Mudflat Microfacies typically have a higher clay mineral content, with some samples exceeding 10%. In contrast, Quiet Water and Tempestite Microfacies contain relatively lower amounts of clay minerals, with some samples showing almost no clay content. This difference in mineral composition reflects variations in the source and postdepositional transformation of clay minerals across different depositional environments. As shown in Table 2, the Mudflat Microfacies samples (depths 4829.15, 4591.66 m) exhibit effective porosity values of around 1.2%, extremely low permeability, and displacement pressures ranging from 27.55 to 41.24 MPa. The low porosity and high displacement pressures are largely attributed to the cementation effect of clay minerals. During cementation, fine clay particles fill the pores between sediment grains, forming a compact cement matrix. This not only compresses primary pores but also reduces the pore throat size, limiting fluid flow (Figure 14).

In contrast, in the Quiet Water Microfacies, the lower-energy depositional environment results in a more dispersed distribution of clay minerals, leading to a less pronounced cementation effect. Although porosity in these samples ranges from 1 to 3%, some permeability is still preserved. In the Tempestite Microfacies, where coarse-grained material predominates, cementation occurs, but the impact on reservoir connectivity is limited due to smaller primary pores and lower clay mineral content. Overall, the cementation effect of clay minerals in the Fengcheng Formation exhibits regional variations across different microfacies. It is most pronounced in Mudflat Microfacies, where pore occlusion and reduced fluid mobility are significant. In the Quiet Water and Tempestite Microfacies, the lower clay content reduces the negative impact of cementation on the reservoir properties.

The carbonate mineral content in the Mudflat Microfacies shows significant variability, ranging from approximately 5−39%, whereas the carbonate content in the Quiet Water and Tempestite Microfacies is comparatively low. This variation reflects differences in the source and depositional control of carbonate minerals across various sedimentary environments. As shown in Table 2, the low porosity and high displacement pressures observed in Mudflat Microfacies samples (depths 4591.66, 4829.15 m) are strongly associated with the high degree of carbonate cementation. In these samples, a high concentration of carbonate minerals acts as a cement during early diagenesis, effectively filling intergranular pores and forming a compact reservoir structure that significantly reduces both porosity and permeability. In contrast, the lower carbonate content in the Quiet Water Microfacies results in less pronounced cementation, allowing for relatively better preservation of the pore throat size and connectivity. The Tempestite Microfacies, however, exhibit more diverse characteristics: while some samples (4848.6 m) still show evidence of carbonate cementation, resulting in higher displacement pressures (34 MPa), others (4783.1 m) demonstrate substantial secondary porosity development, with a significant increase in maximum pore throat radius and a reduction in displacement pressure to as low as 13.77 MPa. These observations suggest that postdepositional carbonate dissolution may have partially alleviated the

https://doi.org/10.1021/acs.energyfuels.4c06392
Energy Fuels 2025, 39, 7235−7253

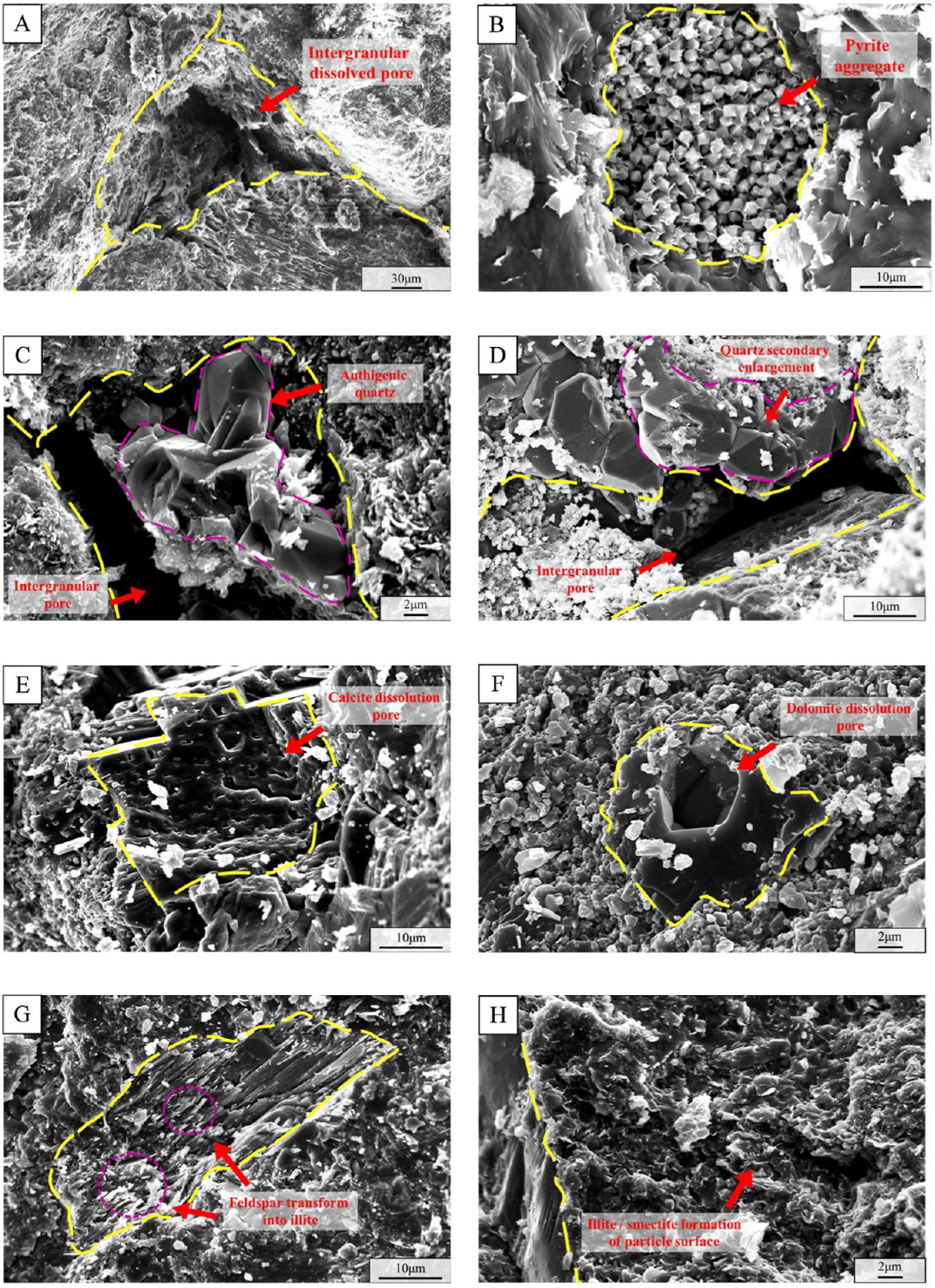

Figure 14. (A) Interparticle dissolution pore JL34 3349 m. (B) Intergranular pyrite aggregate JL35 4526.62 m. (C) Intergranular authigenic quartz MH15 3815.64 m. (D) Quartz secondary enlargement in intergranular pore X77 2339.51 m. (E) Dissolution pores in calcite grains FN4 4403.71 m. (F) Dissolution pores in dolomite grains FN4 4403.71 m. (G) Feldspar transform into Illite FC1 4276.11 m. (H) Irregular illite/smectite formation of particle surface FC1 5456.98 m.

negative effects of early cementation, thus enhancing reservoir connectivity.

5.3.3. Impact of Dissolution on Reservoir Pore Structure. The Fengcheng Formation exhibits significant heterogeneity across different microfacies in response to dissolution. For example, Tempestite Microfacies show considerable variation in their petrophysical properties. A sample at a depth of 4848.6 m has an effective porosity of approximately 6.44% and a permeability of 0.0234 mD, while another sample at 4783.1 m has larger pore throat sizes (with a maximum pore throat radius of 0.053 mm and an average pore throat radius of 0.014 mm) and extremely low displacement pressure. This suggests that postdepositional fluid activity has caused significant dissolution of carbonates and some cementing materials, creating a

https://doi.org/10.1021/acs.energyfuels.4c06392
Energy Fuels 2025, 39, 7235−7253

Table 2. Reservoir Structural Parameters for Different Sedimentary Microphases

number	microfacies	depth/m	penetration/mD	porosity/%	maximum pore throat radius/μm	average pore throat radius/μm	displacement pressure/MPa
1	quiet water	4858.41	0.000429	3.268	0.021	0.008	34.373
2	quiet water	4776.66	0.000217	1.898	0.021	0.008	34.366
3	slump	4690.85	0.000118	1.612	0.018	0.007	41.231
4	slump	4709.68	0.000000435	1.694	0.018	0.007	41.244
5	tempestite	4783.10	0.0184	6.533	0.053	0.014	13.773
6	tempestite	4848.60	0.0234	6.443	0.021	0.008	34.371
7	mudfat	4591.66	0.000124	1.129	0.018	0.007	41.241
8	mudfat	4829.15	0.0000801	1.204	0.027	0.010	27.545

secondary pore system with good connectivity, which in turn enhances reservoir quality. In contrast, the Mudflat and Slump Microfacies show a more limited response to dissolution. Due to stronger early compaction and cementation, these sediments exhibit relatively compact pore systems. Although dissolution can locally improve the pore structure, its overall impact is limited, as evidenced by higher displacement pressures and minimal increases in porosity and permeability. The Quiet Water Microfacies falls in between, with a low-energy depositional environment conducive to mild dissolution. However, the higher degree of early cementation restricts improvements in pore connectivity, resulting in moderate increases in the effective porosity and permeability, which remain at middle to low levels.

5.3.4. Mechanisms of Organic Matter Pore Formation. The formation of organic matter pores in the Fengcheng Formation is influenced by the type of organic matter, thermal maturation, and diagenesis. The organic matter in the Fengcheng Formation is primarily Type II kerogen, which has a high hydrogen content.[42] During pyrolysis, this organic matter primarily generates small molecules of oil and gas, accompanied by the formation of nanometer-scale intergranular pores. These pores are typically distributed between organic matter particles, forming fine micropores rather than larger intraparticle pores. As burial progresses, the Fengcheng Formation undergoes compaction, cementation, and dissolution. In the Quiet Water Microfacies, intense mechanical compaction and cementation by carbonate and clay minerals significantly reduce the primary pore volume, further restricting pore formation. Moreover, the strawberry-like aggregates of pyrite provide some support for intergranular pores but fail to effectively preserve pore connectivity, which is compromised due to cementation.[43] During diagenesis, alkaline hydrothermal activity promotes the interaction between organic matter and clay minerals, resulting in the encapsulation of organic pores by clay minerals. This process further limits pore development and reduces both the porosity and permeability, making the generation of organic pores increasingly complex. Early stage calcite cementation and pyrite precipitation have partially preserved some intergranular pores, but overall, diagenesis has inhibited pore development.

5.4. Sedimentary Microfacies Model. The sedimentary microfacies and pore characteristics of the Fengcheng Formation are closely related. Based on varying depositional environments, the shale of the Fengcheng Formation can be categorized into Quiet Water, Tempestite, Mudflat, and Slump Microfacies. The Quiet Water Microfacies predominantly forms in low-energy, oxygen-deficient environments, exhibiting higher porosity (1%−6%) but lower permeability, with pores primarily consisting of micropores. The Tempestite Microfacies forms under high-energy hydrodynamic conditions, resulting in higher porosity and better permeability. The Mudflat Microfacies has lower porosity (<1.2%) and extremely low permeability, with a more compact pore structure. The Slump Microfacies has lower porosity, poor pore connectivity, and pores primarily concentrated in the medium to small pore size range. Changes in depositional environment significantly influence reservoir pore structure. Shallow water environments promote the formation of Tempestite Microfacies, which exhibit higher porosity but lower permeability. In contrast, deep-water environments favor the formation of Quiet Water Microfacies, where the generation of pyrite helps inhibit compaction, thereby preserving primary porosity. High-salinity environments enhance porosity, while low-salinity environments reduce pore connectivity through the increased presence of clay minerals. Weak oxidative−reductive conditions encourage the formation of pyrite, which further improves pore connectivity.

Furthermore, mineral composition plays a dual role in the evolution of the pore structure. Clay minerals reduce pore connectivity through compaction and cementation, while carbonate minerals generate secondary porosity through dissolution, significantly increasing the complexity of the pore network. Diagenesis, through various physical and chemical processes, further modifies the pore system, especially through compaction, cementation, and dissolution, which have a profound impact on porosity, permeability, and hydrocarbon storage capacity (Figure 15).

6. CONCLUSIONS

(1) The sedimentary microfacies of the Fengcheng Formation are classified into four types: Quiet Water Microfacies, Tempestite Microfacies, Mudflat Microfacies, and Slump Microfacies. The Quiet Water Microfacies forms in low-energy, oxygen-depleted depositional environments, predominantly consisting of fine-grained clayey deposits. The Tempestite Microfacies develops under high-energy conditions, characterized by the accumulation of coarse-grained material, reflecting sedimentary features associated with intense hydrodynamic processes. The Mudflat Microfacies is influenced by biological disturbance and oxidation in low-energy settings, exhibiting significant heterogeneity. The Slump Microfacies results from slope instability, displaying typical soft-sediment deformation structures.

(2) The pore characteristics of the reservoirs vary significantly across different sedimentary microfacies. The Quiet Water Microfacies exhibits relatively high porosity (1−6%) but low permeability, with pores primarily composed of micropores. The Tempestite Microfacies shows superior pore characteristics, with a broad pore size distribution and higher porosity and permeability. The

https://doi.org/10.1021/acs.energyfuels.4c06392
Energy Fuels 2025, 39, 7235−7253

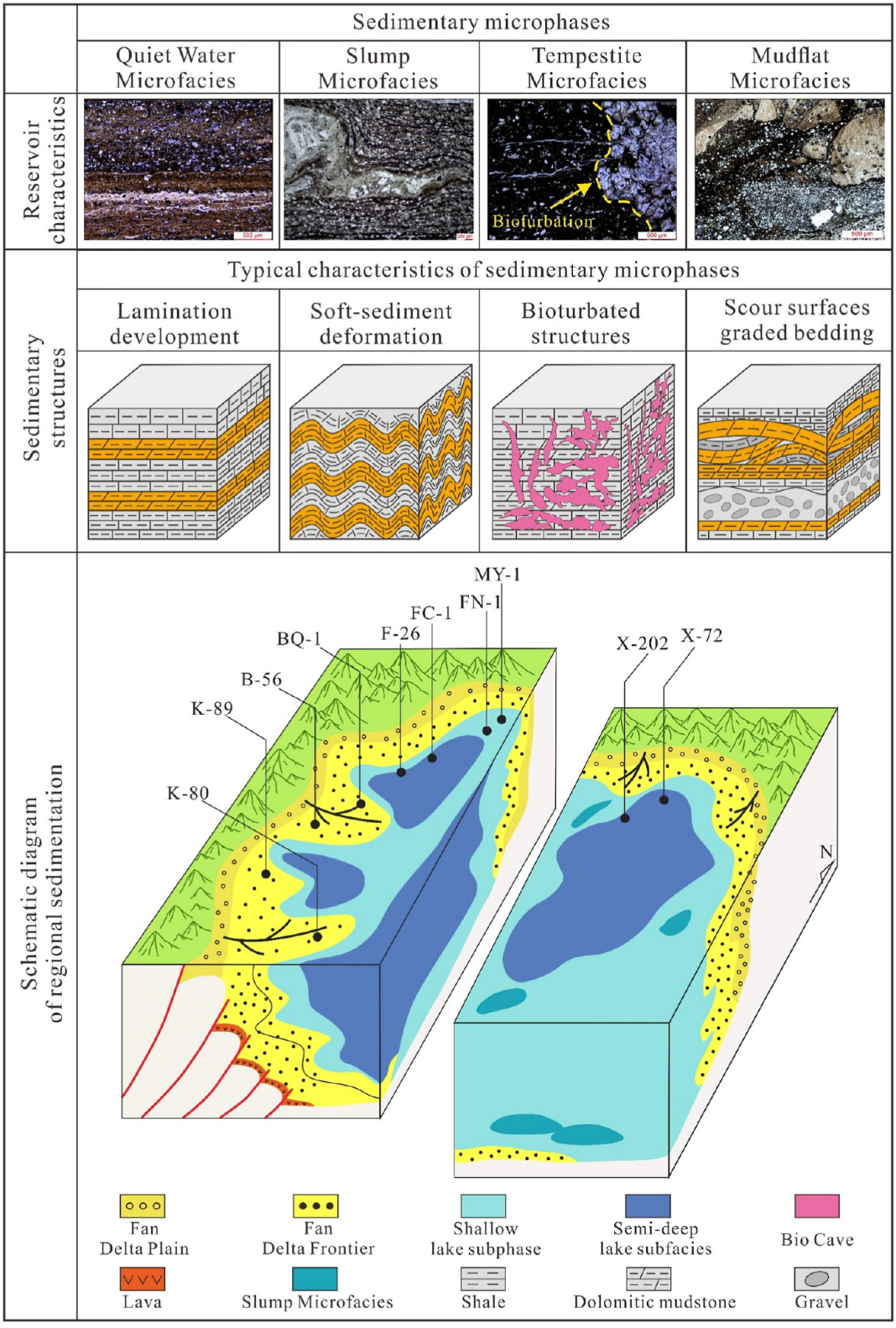

Figure 15. Schematic diagram of the Fengcheng formation sedimentary system.

Mudflat Microfacies has relatively low porosity (<1.2%) and extremely low permeability, with a dense pore structure. The Slump Microfacies is characterized by low porosity, poor pore connectivity, and a pore size predominantly concentrated in the small to medium range.

(3) Depositional environment variations significantly influence reservoir petrophysical properties. Shallow water environments favor the formation of Tempestite Microfacies, which are characterized by high porosity but low permeability. In contrast, deep water environments promote the development of Quiet Water

https://doi.org/10.1021/acs.energyfuels.4c06392
Energy Fuels 2025, 39, 7235−7253

Microfacies, where pyrite formation inhibits compaction and preserves primary porosity. High salinity environments enhance porosity, whereas low salinity environments reduce pore connectivity through the formation of clay minerals. Weakly reducing conditions facilitate pyrite formation, which improves pore connectivity. Mineral composition has a dual impact on pore structure: clay minerals limit pore connectivity through compaction and cementation, while carbonate minerals enhance pore network complexity by dissolution, generating secondary porosity. Diagenesis, including processes such as compaction, cementation, and dissolution, reshapes the pore system, ultimately influencing hydrocarbon accumulation and fluid conductivity.

■ ASSOCIATED CONTENT

Supporting Information

The Supporting Information is available free of charge at https://pubs.acs.org/doi/10.1021/acs.energyfuels.4c06392.

Highlights (PDF)

■ AUTHOR INFORMATION

Corresponding Author

Dongxia Chen − *State Key Laboratory of Petroleum Resources and Engineering, China University of Petroleum, Beijing 102249, China; College of Geosciences, China University of Petroleum, Beijing 102249, China;* orcid.org/0000-0003-4657-9081; Email: lindachen@cup.edu.cn

Authors

Zaiquan Yang − *State Key Laboratory of Petroleum Resources and Engineering, China University of Petroleum, Beijing 102249, China; College of Geosciences, China University of Petroleum, Beijing 102249, China*

Xianglu Tang − *State Key Laboratory of Petroleum Resources and Engineering, China University of Petroleum, Beijing 102249, China; Unconventional Oil and Gas Science and Technology Institute, China University of Petroleum, Beijing 102249, China*

YuChao Wang − *State Key Laboratory of Petroleum Resources and Engineering, China University of Petroleum, Beijing 102249, China; College of Geosciences, China University of Petroleum, Beijing 102249, China*

Zhenxue Jiang − *State Key Laboratory of Petroleum Resources and Engineering, China University of Petroleum, Beijing 102249, China; Unconventional Oil and Gas Science and Technology Institute, China University of Petroleum, Beijing 102249, China;* orcid.org/0000-0002-1936-5494

Leilei Yang − *State Key Laboratory of Petroleum Resources and Engineering, China University of Petroleum, Beijing 102249, China; Unconventional Oil and Gas Science and Technology Institute, China University of Petroleum, Beijing 102249, China*

Zhiye Gao − *State Key Laboratory of Petroleum Resources and Engineering, China University of Petroleum, Beijing 102249, China; Unconventional Oil and Gas Science and Technology Institute, China University of Petroleum, Beijing 102249, China*

Complete contact information is available at: https://pubs.acs.org/10.1021/acs.energyfuels.4c06392

Notes

The authors declare no competing financial interest.

■ ACKNOWLEDGMENTS

We thank PetroChina Xinjiang Oilfield Company for providing samples and data access. This study is supported by Natural Science Foundation of Xinjiang Uygur Autonomous Region (2024D01E09); The Strategic Cooperation Technology Projects of CNPC and CUPB (ZLZX2020-01-05), the National Natural Science Foundation of China (grant nos. 41802153 and 41872135), and the National Major Science and Technology Projects of China (no. 2016ZX05034001-005). We sincerely appreciate all anonymous reviewers and the handling editor for their comments and suggestions.

■ REFERENCES

(1) Hu, S.; Zhao, W.; Hou, L.; Yang, Z.; Zhu, R.; Wu, S.; Bai, B.; Jin, X. Development potential and technical strategy of continental shale oil in China. *Pet. Explor. Dev.* **2020**, *47* (4), 877−887.

(2) Zhao, W.; Hu, S.; Hou, L.; Yang, T.; Li, X.; Guo, B.; Yang, Z. Types and resource potential of continental shale oil in china and its boundary with tight oil. *Pet. Explor. Dev.* **2020**, *47* (1), 1−11.

(3) Bai, L.-H.; Liu, B.; Du, Y.-J.; Wang, B.-Y.; Tian, S.-S.; Wang, L.; Xue, Z.-Q. Distribution characteristics and oil mobility thresholds in lacustrine shale reservoir: insights from adsorption experiments on samples prior to and following hydrocarbon extraction. *Pet. Sci.* **2021**, *2* (19), 486−497.

(4) Li, Z.; Oyediran, I. A.; Huang, R.; Hu, F.; Du, T.; Hu, R.; Li, X. Study on pore structure characteristics of marine and continental shale in China. *J. Nat. Gas Eng.* **2016**, *33*, 143−152.

(5) Gao, G.; Yang, S. R.; Ren, J. L.; Zhang, W. W.; Xiang, B. L. Geochemistry and depositional conditions of the carbonate-bearing lacustrine source rocks: a case study from the early permian fengcheng formation of well fn7 in the northwestern junggar basin. *J. Pet. Sci. Eng.* **2018**, *162*, 407−418.

(6) Tang, W.; Zhang, Y.; Pe-Piper, G.; Piper, D. J. W.; Guo, Z.; Li, W. Permian rifting processes in the NW Junggar basin, China: implications for the post-accretionary successor basins. *Gondwana Res* **2021**, *98*, 107−124.

(7) Wang, P. F.; Jiang, Z. X.; Ji, W. M.; Zhang, C.; Yuan, Y.; Chen, L.; Yin, L. S. Heterogeneity of intergranular, intraparticle, and organic pores in longmaxi shale in the Siem basin, South China: evidence from sem digital images and fractal and multifractal geometries. *Mar. Pet. Geol.* **2016**, *72*, 122−138.

(8) Zhang, F.; Jiang, Z. X.; Xiao, H. M.; Hu, B.; Chen, P.; Tang, X. L.; Sun, W.; Zhu, L.; Wang, Q. Y. Testing origin of reservoir quality difference of tight sandstones in the Yanchang Formation, Ordos Basin, China. *Mar. Pet. Geol.* **2022**, *137* (3), 105507.

(9) Liu, H. Y.; Shi, K. B.; Liu, B.; Song, X. M.; Guo, R.; Wang, G. J.; Wang, H. Microfacies and reservoir quality of the middle cretaceous rumaila formation in the ad oilfield, central mesopotamian basin, southern iraq. *J. Asian Earth Sci.* **2021**, *213* (5), 104726.

(10) Zhao, N. B.; Ye, J. R.; Yang, B. L.; Zhang, F.; Yu, H. W.; Xu, C. J.; Xu, S. K.; Xu, J. Y.; Shu, Y. Depositional palaeoenvironment and models of the eocene lacustrine source rocks in the northern south china sea. *Mar. Pet. Geol.* **2021**, *128* (2), 105015.

(11) Kim, I. Swinging shale: Shale oil, the global oil market, and the geopolitics of oil. *Int. Stud. Q.* **2020**, *64* (3), 544−557.

(12) Zhang, Y.; Zhang, G.; Zhao, W.; Zhou, J.; Li, K.; Cheng, Z. Total organic carbon content estimation for mixed shale using Xgboost method and implication for shale oil exploration. *Sci. Rep.* **2024**, *14* (1), 20860.

(13) Wu, Y.; Liu, C.; Jiang, F.; et al. Geological characteristics and shale oil potential of alkaline lacustrine source rock in Fengcheng Formation of the Mahu Sag, Junggar Basin, Western China. *J. Pet. Sci. Eng.* **2022**, *216*, 110823.

(14) Finkelstein, D. B.; Hay, R. L.; Altaner, S. P. Origin and diagenesis of lacustrine sediments, upper Oligocene Creede Formation, southwestern colorado. *Geol. Soc. Am. Bull.* **1999**, *111* (8), 1175−1191.
(15) Hatano, N.; Yoshida, K. Sedimentary environment and paleosols of middle Miocene fluvial and lacustrine sediments in central japan: implications for paleoclimate interpretations. *Sediment. Geol.* **2017**, *347* (1), 117−129.
(16) Tang, W.; Zhang, Y.; Pe-Piper, G.; Piper, D. J. W.; Guo, Z.; Li, W. Soft-sediment deformation structures in alkaline lake deposits of Lower Permian Fengcheng Formation, Junggar Basin, NW China: Implications for syn-sedimentary tectonic activity. *Sediment. Geol.* **2020**, *406*, 105719.
(17) Lahann, R. W.; Swarbrick, R. E. Overpressure generation by load transfer following shale framework weakening due to smectite diagenesis. *Geofluids* **2011**, *11* (4), 362−375.
(18) Liu, H.; Zhang, S.; Song, G.; Xuejun, W.; Teng, J.; Wang, M.; Bao, Y.; Yao, S.; Wang, W.; Zhang, S.; Hu, Q.; Fang, Z. Effect of shale diagenesis on pores and storage capacity in the paleogene shahejie formation, dongying depression, bohai bay basin, east china. *Mar. Pet. Geol.* **2019**, *103* (5), 738−752.
(19) Wang, J.; Zhou, L.; Liu, J.; Zhang, X. J.; Zhang, F.; Zhang, B. Z. Acid-base alternation diagenesis and its influence on shale reservoirs in the Permian Lucaogou Formation, Jimusar sag, Junggar Basin, NW China. *Pet. Explor. Dev.* **2020**, *47* (5), 962−976.
(20) Clarkson, C. R.; Solano, N.; Bustin, R. M.; Bustin, A. M. M.; Chalmers, G. R. L.; He, L.; Melnichenko, Y. B.; Radlinski, A. P.; Blach, T. P. Pore structure characterization of north American shale gas reservoirs using usans/sans, gas adsorption, and mercury intrusion. *Fuel* **2013**, *103*, 606−616.
(21) Shao, X. H.; Pang, X. Q.; Li, Q. W.; Wang, P. W.; Chen, D.; Shen, W. B.; Zhao, Z. F. Pore structure and fractal characteristics of organic-rich shales: a case study of the lower silurian longmaxi shales in the Shuan basin, SW China. *Mar. Pet. Geol.* **2017**, *80*, 192−202.
(22) Gao, Z.; Liang, Z.; Qinhong, H.; Jiang, Z.; Xuan, Q. A new and integrated imaging and compositional method to investigate the contributions of organic matter and inorganic minerals to the pore spaces of lacustrine shale in china. *Mar. Pet. Geol.* **2021**, *127* (6), 104962.
(23) Tang, Y.; Cao, J.; He, W. J.; Guo, X. G.; Zhao, K. B.; Li, W. W. Discovery of shale oil in alkaline lacustrine basins: the late paleozoic Fengcheng formation, Mahu sag, Junggar basin, China. *Pet. Sci.* **2021**, *18* (5), 1281−1293.
(24) Imin, A.; Zha, M.; Ding, X. J.; Bian, B. L.; Liu, Y.; Zheng, M. L.; Han, C. Identification of a permian foreland basin in the western Junggar basin (north China) and its impact on hydrocarbon accumulation. *J. Pet. Sci. Eng.* **2020**, *187*, 106810.
(25) Mao, X.; Li, J.; Zhang, H.; Wang, L. Study on the distribution and developmental environment of the late paleozoic volcanoes in junggar basin and its adjacent areas. *Acta Petrol. Sin.* **2012**, *28* (8), 2381−2391.
(26) Wang, Y. J.; Jia, D.; Pan, J. U.; Wei, D. T.; Tang, Y.; Wang, G. D.; Wei, C. R.; Ma, D. L. Multiple-phase tectonic superposition and reworking in the junggar basin of northwestern china-implications for deep-seated petroleum exploration. *AAPG Bulletin* **2018**, *102* (8), 1489−1521.
(27) Gao, Z. Y.; Hu, Q. H. Pore structure and spontaneous imbibition characteristics of marine and continental shales in china. *AAPG Bulletin* **2018**, *102* (10), 1941−1961.
(28) Zhang, Z. J.; Yuan, X. J.; Wang, M. S.; Zhou, C. M.; Tang, Y.; Chen, X. Y.; Lin, M. J.; Cheng, D. W. Alkaline-lacustrine deposition and paleoenvironmental evolution in permian fengcheng formation at the mahu sag, junggar basin, nw china. *Pet. Explor. Dev.* **2018**, *45* (6), 1036−1049.
(29) Feng, Y.; Zhang, Y.; Wang, R.; Zhang, G.; Wu, W. Dolomites genesis and hydrocarbon enrichment of the Fengcheng Formation in the northwestern margin of Junggar Basin. *Pet. Explor. Dev.* **2011**, *38* (6), 685−692.
(30) Zhi, D.; Tang, Y.; He, W.; Guo, X.; Zheng, M.; Huang, L. Orderly coexistence and accumulation models of conventional and unconventional hydrocarbons in Lower Permian Fengcheng Formation, Mahu sag, Junggar Basin. *Pet. Explor. Dev.* **2021**, *48* (1), 43−59.
(31) Zhao, P. Q.; Wang, Z. L.; Sun, Z. C.; Cai, J. C.; Wang, L. Investigation on the pore structure and multifractal characteristics of tight oil reservoirs using nmr measurements: permian lucaogou formation in jimusaer sag, junggar basin. *Mar. Pet. Geol.* **2017**, *86*, 1067−1081.
(32) Xi, K. L.; Cao, Y. C.; Haile, B. G.; Zhu, R. K.; Jahren, J.; Bjorlykke, K.; Zhang, X. X.; Hellevang, H. How does the pore-throat size control the reservoir quality and oiliness of tight sandstones? In the case of the lower cretaceous quantou formation in the southern Songliao basin, China. *Mar. Pet. Geol.* **2016**, *76*, 1−15.
(33) Lai, J.; Wang, G.; Fan, Z.; Chen, J.; Wang, S.; Zhou, Z.; Fan, X. Insight into the pore structure of tight sandstones using nmr and hpmi measurements. *Energy Fuels* **2016**, *30* (12), 10200−10214.
(34) Curtis, M. E. Structural characterization of gas shales on the micro-and nano-scales, *Canadian Unconventional Resources and International Petroleum Conference*. Society of Petroleum Engineers, 2010; p 137693.
(35) Sondergeld, C. H.; Ambrose, R. J.; Rai, C. S.; Moncrieff, J. Microstructural Studies of Gas Shales; *SPE Unconventional Resources Conference/Gas Technology Symposium*. Society of Petroleum Engineers, 2010; p 131771.
(36) Chen, L.; Jiang, Z. X.; Liu, K. Y.; Tan, J. Q.; Gao, F. L.; Wang, P. F. Pore structure characterization for organic-rich lower silurian shale in the upper yangtze platform, south china: a possible mechanism for pore development. *J. Nat. Gas Eng.* **2017**, *46*, 1−15.
(37) Wang, X.; Li, J.; Huang, Y.; et al. Influence of Paleosedimentary Environment on Shale Oil Enrichment in the Raoyang Sag, Bohai Bay Basin. *Energy Fuels* **2022**, *36* (22), 13597−13616.
(38) Sethi, C.; Hazra, B.; Ostadhassan, M.; et al. Depositional environmental controls on mechanical stratigraphy of Barakar Shales in Rajmahal Basin, India. *Int. J. Coal Geol.* **2024**, *285*, 104477.
(39) Boboye, O. A.; Jaiyeoba, O. K.; Okon, E. E. Sedimentological characteristics and mineralogical studies of some Cretaceous sandstones in Nigeria: Implications for depositional environment and provenance. *J. Sediment. Environ.* **2021**, *6* (4), 531−550.
(40) MacKenzie, F. T. Diagenesis of Shaly Rocks. *AAPG Bulletin* **1970**, *54* (5), 858.
(41) Charlton, T. S.; Goodarzi, M.; Rouainia, M.; Aplin, A. C.; Cubillas, P. Effect of diagenesis on geomechanical properties of organic-rich calcareous shale: A multiscale investigation. *J. Geophys. Res. Solid Earth* **2021**, *126* (7), No. e2020JB021365.
(42) Wang, X.; Gao, J.; Zhong, L.; et al. The volcanic impacts on the formation of organic-rich shales from the freshwater to saline lakes: Cases study in the Ordos and the Junggar basins. *Front. Earth Sci.* **2022**, *10*, 918391.
(43) Carcione, J. M.; Gei, D.; Picotti, S.; et al. Rock acoustics of diagenesis and cementation. *Pure Appl. Geophys.* **2022**, *179* (5), 1919−1934.

https://doi.org/10.1021/acs.energyfuels.4c06392
Energy Fuels 2025, 39, 7235−7253